Zhou *et al. Journal of Neuroinflammation* (2025) 22:134
https://doi.org/10.1186/s12974-025-03466-8

Journal of Neuroinflammation

RESEARCH Open Access

Caveolin-1 negatively regulates the calcitonin receptor-like receptor and neuroinflammation in a female mouse model of migraine

Yanjie Zhou[1†], Wu Chen[2†], Yu Zhang[1], Liu Yang[1,3], Fu Lu[1], Wen Yan[1], Qingfang Xie[1], Ying Huang[1], Wanbin Huang[1], Lintao Wang[1], Ziming Zeng[1] and Zheman Xiao[1*]

Abstract

Background Caveolin-1 (CAV1), a scaffolding protein critical for caveolae formation, regulates G-protein-coupled receptor (GPCR) signaling via caveolae-mediated endocytosis. The calcitonin receptor-like receptor (CLR), a GPCR and core subunit of the calcitonin gene-related peptide (CGRP) receptor, is a therapeutic target for migraine. However, the role of CAV1 in CLR regulation and migraine remains unclear.

Methods A migraine model was established in female mice via dural inflammatory soup (IS) application. Migraine-like behaviors were assessed using Von Frey filament, spontaneous pain behavior counts, light/dark box, and acetone test. CAV1 was overexpressed by lentivirus and downregulated by small interfering RNA (siRNA) technology. Methyl-β-cyclodextrin (MβCD) was used to inhibit caveolae-mediated endocytosis. The molecular mechanism of CAV1 on CLR and neuroinflammation was investigated using biochemistry, multiplex immunohistochemistry staining, internalization assay, and co-immunoprecipitation.

Results Repeated IS stimulation elevated CLR expression and internalization in the trigeminal nucleus caudalis (TNC), concurrently activating ERK/CREB signaling, promoting microglial activation, and increasing inflammatory cytokines (TNFα, IL-1β). CAV1 directly interacted with CLR, promoting its degradation. CAV1 knockdown in the TNC exacerbated migraine pathology, characterized by CLR accumulation, enhanced ERK/CREB phosphorylation, and amplified neuroinflammation. Conversely, CAV1 overexpression or MβCD-mediated caveolae disruption normalized CLR levels, reduced signaling hyperactivity, and reversed nociceptive behaviors.

Conclusion CAV1 negatively regulates CLR stability, suppressing ERK/CREB signaling and microglial inflammation in a preclinical female migraine model. These findings suggest that CAV1 contributes to migraine-related hyperalgesia and may represent a novel therapeutic target for migraine treatment.

Keywords Caveolin-1, CLR, Migraine, Microglia, Neuroinflammation

†Yanjie Zhou and Wu Chen contributed equally to this work.

*Correspondence:
Zheman Xiao
zmxiao@whu.edu.cn

[1]Department of Neurology, Renmin Hospital of Wuhan University, Wuhan University, 99 Zhangzhidong Road, Wuhan 430060, China
[2]Department of Urology, Renmin Hospital of Wuhan University, Wuhan University, 99 Zhangzhidong Road, Wuhan 430060, China
[3]Department of Thoracic Surgery, Renmin Hospital of Wuhan University, Wuhan University, 99 Zhangzhidong Road, Wuhan 430060, China

Introduction

Migraine is a prevalent neurovascular disorder disease, predominantly affecting women and often accompanied by nausea, vomiting, photophobia, and phonophobia [1, 2]. According to the Global Burden Disease (GBD) 2021, migraine ranks as the third most disabling neurological disorder [3]. Current therapeutic strategies primarily target the calcitonin gene-related peptide (CGRP) pathway. Four monoclonal antibodies (fremanezumab, galcanezumab, eptinezumab, and erenumab) targeting CGRP or its receptor have been approved for migraine prevention, demonstrating significant efficacy in Phase III clinical trials [4, 5]. The functional CGRP receptor comprises calcitonin receptor-like receptor (CLR) and receptor activity modifying protein 1 (RAMP1) [6]. By binding to and activating its receptor complex, CGRP causes vasodilatation with plasma protein extravasation and meningeal mast cell degranulation during a migraine attack [7]. CLR, the core component of the CGRP receptor complex, undergoes agonist-stimulated internalization with subsequent sorting and trafficking to either lysosomal degradation or plasma membrane recycling [8, 9]. Degradation of CLR attenuates CGRP signaling, mitigating migraine-related pathology, whereas deleterious recycling sustains or amplifies it, potentially worsening migraine [8, 10]. However, the mechanisms underlying the differential trafficking and outcomes of CLR internalization remain to be determined.

Caveolin-1 (CAV1) is a 22 kDa intracellular protein that is a major component associated with small nested lipid rafts in the plasma membrane [11]. CAV1 involves multiple cellular processes, including cell growth, differentiation, endocytosis, cholesterol trafficking, and cellular senescence [12]. Many studies pointed to caveolae and caveolins as important regulators of G-protein-coupled receptor (GPCR) traffic and function [13, 14]. GPCR agonists can enrich receptors in caveolae or do the opposite [15, 16]. Caveolae, CAV1, GPCR, and even G protein-coupled receptor kinases (GRKs) may be jointly regulated downstream signaling pathways through complex mechanisms [13]. CAV1 modulates cell surface signaling through diverse mechanisms involving caveolae-dependent pathways [17]. For instance, Raf-1 is recruited to caveolae upon EGF stimulation, which is essential for MAP kinase pathway activation [18], whereas caveolae may be depleted of certain membrane proteins under different conditions [19]. This functional diversity indicates that CAV1 can direct receptor trafficking fates. Nevertheless, little is known about the mechanism of CAV1-CLR interaction and the effect of the interaction on CLR internalization.

Previous studies suggest that neuroinflammatory changes, including microglia activation, are key pathological components of migraine [20, 21]. The interaction between neurons and microglia affects the transmission of pain signals [20]. In addition to interacting with GPCRs, CAV1 appears to be a critical component of microglia and regulating upstream/downstream regulatory elements in inflammation [22]. Studies have shown that CAV1 can negatively regulate the inflammatory response, which is considered a neuroprotective factor, and that lack of CAV1 enhances neuroinflammation [23, 24]. However, CAV1 has been little studied in migraine, and the specific molecular mechanisms and signaling pathways remain unknown.

This research aimed to explore the role of CAV1 in migraine using in vitro and in vivo experiments. In particular, we investigated the mechanisms of CAV1 interactions with CLR, identified proteins involved in the process, and assessed microglial-mediated inflammation.

Materials and methods

Animals and groups

Female C57BL/6 mice weighing 17-19 g between seven and eight weeks of age were used in the study. All mice used in this experiment were provided by Hunan Slake Jingda Experimental Animal Co., Ltd. Mice were housed in a controlled environment with a standard 12:12 light-dark cycle, temperature of 19-22 °C, and humidity of 50-55% and free access to food and water. All experiments were conducted in consideration of the fundamental ethical principles of animal experiments and the "3R" principles. The in vivo animal study consisted of five experiments, with mice grouped in each section as follows. Experiment 1: (1) PBS, (2) IS; Experiment 2: (1) PBS-vehicle (VEH), (2) PBS-BIBN4096, (3) IS-VEH, (4) IS-BIBN4096; Experiment 3: (1) normal control (NC), (2) siRNA-CAV1(si-CAV1); Experiment 4: (1) PBS-VEH, (2) PBS-MβCD, (3) IS-VEH, (4) IS-MβCD; Experiment 5: (1) lentivirus (LV)-NC + PBS, (2) LV-NC + IS, (3) LV-CAV1 + IS. Eight mice per group were utilized. Mice were randomly assigned throughout the whole trial. All mice were acclimated for one week before the initiation of experiments.

Establishment of a migraine mouse model

A mouse model of migraine was induced by repeated dural infusions of inflammatory soup (IS) as described previously [25]. IS stimulates the dura mater by inducing sterile inflammation, thereby causing migraine-like behavior in mice. Mice were anesthetized with 3% isoflurane for induction and 1.5% isoflurane for maintenance. An incision in the midline of the scalp was made to expose the skull. A small hole (diameter = 1 mm) was drilled into the skull at 1 mm posterior and 1 mm lateral to bregma, leaving the dura intact. One guide cannula was implanted to allow microinjections. After surgery, the incision was sutured, and erythromycin ointment

was topically used to prevent infection. Dural injection of IS was conducted one week following recovery from surgery. IS consists of 2 mM prostaglandin E2, 2 mM serotonin, 2 mM histamine and 2 mM bradykinin. IS was injected into the guide cannula using a microinjector with an injection volume of 20 μl daily for 7 days. Controls were injected with equal phosphate buffer saline (PBS).

Behavioral tests

Behavioral tests were conducted prior to euthanasia by an experimenter blinded to the experimental conditions.

Mechanical pain threshold

The mechanical threshold was measured using von Frey filaments as previously described [26]. Mice were acclimated to the testing box 30 min prior to the test. Von Frey filaments were gently pressed onto the periorbital region, sufficient force was applied to bend the filament, and the contact was maintained for 1-2 s. The positive response was defined as sudden head withdrawal, scratching, and shaking. A smaller filament was used when a positive response appeared; otherwise, a larger filament was used. The smallest force that elicited withdrawn responses was recorded.

Spontaneous pain-related behaviors

Spontaneous behaviors, including head-scratching and freezing, were recorded in plexiglass cages where mice could move freely. Mice usually exhibit discomfort and pain in the head and periorbital region under migraine conditions. Head-scratching behavior can be used to assess the effectiveness of migraine models, which typically refers to the forepaws of mice scratching the scalp and periorbital skin area [27]. The number of head-scratching was counted during the 1-hour period immediately after the last drug administration. Freezing refers to the state in which the mouse stops activities and remains still [28]. Freezing time immediately after the last drug administration within 5 min was also recorded.

Cold pain threshold

Cold allodynia was assessed using the acetone test. Mice were placed in a transparent plastic box and given 30 min for habituation. Then, one drop of acetone was applied to the periorbital region. The behaviors of mice after the acetone spray were monitored and scored according to the following criteria: 0 for no response, 1 for mild head withdrawal or flicking, 2 for prolonged and rapid head shaking, and 3 for scratching or rubbing head. The total score of mice showing a positive response within 1 min was recorded.

Photophobia behavior

Photophobia was assessed by calculating time spent in the light during a light/dark box test according to published methods [29]. The light/dark box apparatus comprises two equally connected compartments: light and dark (each containing 30 × 30 × 20 cm). At the beginning of the experiment, the mice were placed near the hole in the center of the box and allowed to explore freely for 5 min. The movement trajectory of mice was automatically detected.

Cell culture and treatment

SH-SY5Y cells are a widely used human neuroblastoma cell line. BV2 cells are an immortalized murine microglial cell line. SH-SY5Y and BV2 cells were purchased from Procell Life Science & Technology Co, Ltd (Procell, Wuhan, China) and cultured in RPMI 1640 medium with 10% fetal bovine serum (FBS), 100 U/ml penicillin, and 100 μg/ml streptomycin at 37℃ and 5% CO_2. To assess the effects of CGRP on CAV1, SH-SY5Y cells were treated with various concentrations of CGRP (1, 3, 5, 10, and 20 μM) for 1 h, while control cells were treated with PBS.

Plasmids, siRNA, and transfection

The human CLR ORF with a Myc tag (pCMV-CAL-CRL), CAV1 ORF with a Flag tag (pLV3-CMV-CAV1), and empty vector plasmid (pCMV-MCS-3×MYC, pCMV-MCS-3×Flag) were constructed by Miaoling Biology (Wuhan, China). Three methoxy-2-tetralone and cholesterol-modified siRNA constructs targeting mouse CAV1 (siRNA1: forward, 5′-GCUUCCUGAUUGAmGAUUCAGUdTdT-3′, reverse, 5′-ACUGAAUCUCAAUCAGGAAGCdTdT-3′; siRNA2: forward, 5′-CGACGUGGUCAAGAUUGACUUdTdT-3′, reverse, 5′-AAGUCAAUCUUGACCACGUCGdTdT-3′; and siRNA3: forward, 5′-CCGCUUGUUGUCUACGAUCUUdTdT-3′, reverse, 5′-AAGAUCGUAGACAACAAGCGGdTdT-3′) and a negative control (siRNA-NC) construct were constructed by Gentle Gen (Suzhou, China). ExFect Transfection Reagent (Vazyme, Nanjing, China) was used to transfect the plasmids and siRNA into SH-SY5Y cells according to the manufacturer's instructions. Cells were collected for subsequent experiments 36-48 h following transfection.

siRNA in vivo transfection

The RNase-free water and in vivo transfection reagent were used to dissolve siRNA, reaching the final concentration of 2 μmol/l. For in vivo transfection, 10 μl of the diluted siRNA solution and Entranster in vivo transfection reagent Engree Biosystems Co., Beijing, China) were mixed according to the manufacturer's instructions. The mixed solution was microinjected into the trigeminal

nucleus caudalis (TNC) immediately (AP: -7.78 mm; DV: -4.75 mm; ML: ±1.65 mm) [30]. The injection site was confirmed by injecting a red fluorescent dye DiI (0.8 μl; Fig. 5c). The injection was repeated after two days to obtain a more stable transfection effect. Behavioral tests and animal sacrifices were conducted two days after the second injection.

Inhibition of caveolin-mediated endocytosis

Methyl-β-cyclodextrin (MβCD) was used to disrupt caveolin-mediated endocytosis by depleting cholesterol from lipid rafts [31]. In cell experiments combined with CGRP, SH-SY5Y cells were pre-treated with 1 μM CGRP for 1 h to activate CLR and ensure functional CGRP receptor expression without altering CAV1 levels. Cells were then treated with 5 mM MβCD (MCE, HY-101461) dissolved in a mixture of 10% DMSO, 40% PEG300, 5% Tween80, and 45% saline for 30 min [32]. Control cells received the same volume of solvent.

For animal experiments, nasal injection has been widely used in the treatment of migraine as a non-invasive way of administering drugs to the brain, which can effectively cross the blood-brain barrier and increase the concentration of drugs entering the brain [33–35]. To test the therapeutic effect of MβCD on migraine, MβCD (10 μl, 1 μg/μl) was given intranasally every day after IS or PBS treatment according to the manufacturer's recommendations.

BIBN4096 treatment

The CGRP receptor antagonist BIBN4096 was freshly dissolved in a vehicle solution consisting of 10% DMSO, 40% PEG300, 5% Tween80, and 45% saline and administered intranasally (10 μl, 0.01 μg/μl) within 30 min following each IS injection. The administration dosage was determined based on previous studies [36].

Lentiviral production and transduction

Human and mouse CAV1 overexpression lentiviruses (pLV3-CMV-CAV1) and control lentiviral vectors were synthesized by Miaoling Biology (Wuhan, China). For lentiviral transduction, SH-SY5Y cells were infected with pLV3-CMV-CAV1 (human) at a multiplicity of infection (MOI) of 100 for 72 h at 37 °C and 5% CO_2 to establish a CAV1 overexpression cell line. Transduction efficiency was confirmed by Western blot analysis. To assess the effect of neuronal CAV1 overexpression on microglia, the conditioned medium was collected from CAV1-overexpressing and control cell lines and used to culture BV2 cells for 24 h, after which cell lysates were harvested for inflammatory factor detection.

To investigate the role of CAV1 in vivo, 5 μl control lentivirus or CAV1 overexpression lentivirus (pLV3-CMV-CAV1 (mouse), 10^9 TU/ml) was microinjected into the TNC according to the manufacturer's instructions. Migraine modeling was performed one week after the lentivirus injection.

Cell membrane and cytosol protein isolation

The TNC tissue of mice and SH-SY5Y cells were harvested. The membrane and cytosol proteins were isolated using a Membrane and Cytosol Protein Extraction Kit (P0033, Beyotime, Shanghai). The pellet was collected for further studies.

Western blot (WB) analysis

Mice brain tissue or cell samples were lysed in RIPA buffer containing phenylmethylsulfonyl fluoride (PMSF) and a protease inhibitor cocktail. Protein samples were separated using 10% or 12.5% SDS-PAGE and then transferred onto a polyvinylidene-difluoride (PVDF) membrane (Millipore, USA). After blocking with a blocking solution (PS108P, Epizyme, Shanghai) for 20 min, the membranes were incubated with primary antibody overnight at 4 °C. Primary antibodies used were as follows: CLR (1:500, A8533, Abclonal), Caveolin-1 (1:1000, 16447-1-AP, Proteintech), DYKDDDDK (1:20000, 20543-1-AP, Proteintech), MYC (1:3000, 16286-1-AP, Proteintech), NaK ATPase (1:1000, 3010S, Cell Signaling Technology), ERK1/2 (1:1000, AF1015, Affinity Biosciences), pERK1/2 (1:1000, 16286-1-AP, Affinity Biosciences), pCREB (1:1000, A99875, HY CEZMBIO), CREB (1:1000, A34072, HY CEZMBIO), TNFα (1:500, GB115701, Servicebio), IL-1β (1:500, GB11113, Servicebio), GAPDH (1:1000, 10494-1-AP, Proteintech). Subsequently, the membrane was washed with TBST and then incubated with HRP-conjugated secondary antibody for 1 h at room temperature. Proteins were detected by an enhanced chemiluminescence (ECL) system. Image J software was used to measure the chemiluminescence intensity of protein bands.

Co-immunoprecipitation (co-IP)

Mice brain tissue or cells were lysed by Western and IP lysis buffer (Beyotime, Shanghai, China), and the co-IP was performed using Protein A/G Magnetic Beads (Selleck, USA). Briefly, lysate (100 μl) was incubated with targeting antibody (CLR, A8533, Abclonal, 10 μg; DYKDDDDK, 20543-1-AP, Proteintech, 2 μg; MYC, 16286-1-AP, Proteintech, 2 μg; IgG, 30000-0-AP, Proteintech, 2 μg) overnight at 4 °C. Then, pretreatment of magnetic beads and incubated with the antibody-antigen complexes for 4 h at 4 °C. Finally, the beads were washed three times with lysis buffer and resuspended in SDS-loading buffer/lysis buffer (1:1). After being heated at 95 °C for 10 min, these samples were analyzed by western blotting. To avoid IgG bands on the IP blot, the non-heavy chain IgG secondary antibody (1:5000, A25022,

Abbkine) and the non-light chain IgG secondary antibody (1:5000, A25122, Abbkine) were used.

Multiplex immunohistochemistry staining (mIHC)

Multiplex immunohistochemistry staining assay was performed according to the previously described protocols [37]. In detail, cell or frozen tissue Sect. (8 μm thick) were fixed with cold acetone for 20 min and then washed three times in PBS for 5 min per wash. Sections were treated with 3% H_2O_2 for 10 min to block endogenous peroxidase activity. After washing with PBS, the sections were blocked with 5% BSA for 45 min at room temperature. Then incubated them with primary antibody (caveolin-1, 1:500, 16447-1-AP, Proteintech; CLR, 1:400, A8533, Abclonal; IBA1, 1:1000, GB15105, Servicebio; c-Fos, 1:500, GB11069, Servicebio; CGRP, 1:500, sc-57053, Santa Cruz), overnight at 4℃. After washing, sections were incubated with an HRP-labeled secondary antibody. CGRP staining was visualized with CY3-Tyramide (G1233, Servicebio) at room temperature for 10 min, while other antigens were stained with Alexa Fluor 488 Tyramide (SB-YT0070, ShareBio) for 10 min at room temperature. Sections were then washed three times with PBS. To strip the antibodies, sections were placed in sodium citrate antigen retrieval solution and microwaved at high heat for 10 min. After cooling to room temperature, sections were blocked in 5% BSA again and incubated with a new primary antibody (CLR, 1:400, A8533, Abclonal; caveolin-1, 1:500, 16447-1-AP, Proteintech) according to experimental needs. Fluorescence intensity was amplified with CY3-Tyramide (G1233, Servicebio). Finally, the DAPI-containing anti-fluorescence quencher was used to seal the glass slides.

Immunofluorescence-based internalization assay

An immunofluorescence-based internalization assay was performed using the method referred to by Thomas et al. [38]. Briefly, after transfected with CALCRL, SH-SY5Y cells were incubated with the CLR antibody for 30 min at 4 °C. After washing the cells extensively with ice-cold PBS, the cells were incubated for 60 min at 37 °C in the presence or absence of drugs (sucrose, 450 μmol/L, Sinopharm Chemical Reagent Co., Ltd); nystatin, 15 mg/ml, Aladdin; amiloride, 1 mmol/l, Aladdin; chlorpromazine, 15 μg/ml, Aladdin). Control cultures were left at 4 °C, a nonpermissive condition for internalization. The cells were rewashed with ice-cold PBS, and then cell surface receptors were labeled with a FITC-conjugated secondary antibody (1:100; Servicebio) for 60 min at 4 °C. Cells were then fixed with 75% ice-cold ethanol for 20 min. For permeabilization, cells were treated with PBS containing 0.5% Triton X-100 for 10 min. Afterward, cells were incubated with Cy3-conjugated secondary antibodies (1:200; Servicebio) for 1 h at room temperature to label the internalized receptors. Finally, the cells were sealed with DAPI-containing anti-fluorescence quenching sealing tablets and observed under a fluorescence microscope (Olympus BX53; Olympus, Japan) to collect images.

Statistical analyses

Statistical analyses were performed with SPSS version 22.0 and GraphPad Prism 8.0.1. All data were presented as mean ± standard error of the mean (SEM). Data sets with normal distributions were analyzed with unpaired Student's two-tailed t-tests to compare two groups and one-way analysis of variance (ANOVA) to compare three or more groups. Post hoc multiple comparisons were conducted using Tukey's test. Non-parametric data were analyzed using the Mann-Whitney test to compare two groups and the Kruskal-Wallis test with the Dunns multiple comparisons test to compare three or more groups. $p < 0.05$ indicated a significant difference.

Results

CAV1 downregulation and CLR upregulation in TNC after repeated IS dural stimulation

To investigate the role of CAV1 in migraine, we established migraine models using repeated IS dural infusions. Compared to PBS-treated controls, IS administration significantly reduced periorbital mechanical thresholds (Fig. 1a) while increasing head-scratching counts (Fig. 1b), freezing time (Fig. 1c), cold pain scores (Fig. 1d), and photophobia behaviors (Fig. 1e-g). Immunofluorescence staining for c-Fos in the TNC revealed a significant increase in c-Fos-positive cells in the IS group compared to the PBS group (Fig. S1a, b), indicating activation of the trigeminovascular system. These behavioral tests and c-Fos immunoreactivity indicated the successful establishment of the migraine model.

Immunofluorescence analyses revealed that repeated IS stimulation upregulated CLR ($p < 0.01$) but downregulated CAV1 fluorescence intensity ($p < 0.001$) in the TNC (Fig. 1h-j). Quantification of CLR-positive cells demonstrated that >70% exhibited partial/complete internalization in IS-treated mice versus <30% in controls (Fig. 1h, l). Corresponding protein changes were confirmed by western blot. CLR increased ($p < 0.05$, Fig. 1m, n) while CAV1 decreased ($p < 0.05$, Fig. 1m, o) in the IS group. Additionally, CGRP levels in the TNC were also elevated after IS stimulation (Fig. S1c, d). These complementary changes in CLR and CAV1 dynamics suggest opposing roles in migraine pathophysiology.

To investigate the functional role of CGRP/CLR signaling in migraine pathophysiology, we administered the CGRP receptor antagonist BIBN4096 to mice subjected to IS-induced dural stimulation. BIBN4096 administration attenuated IS-induced migraine-like behaviors in female mice, evidenced by restored

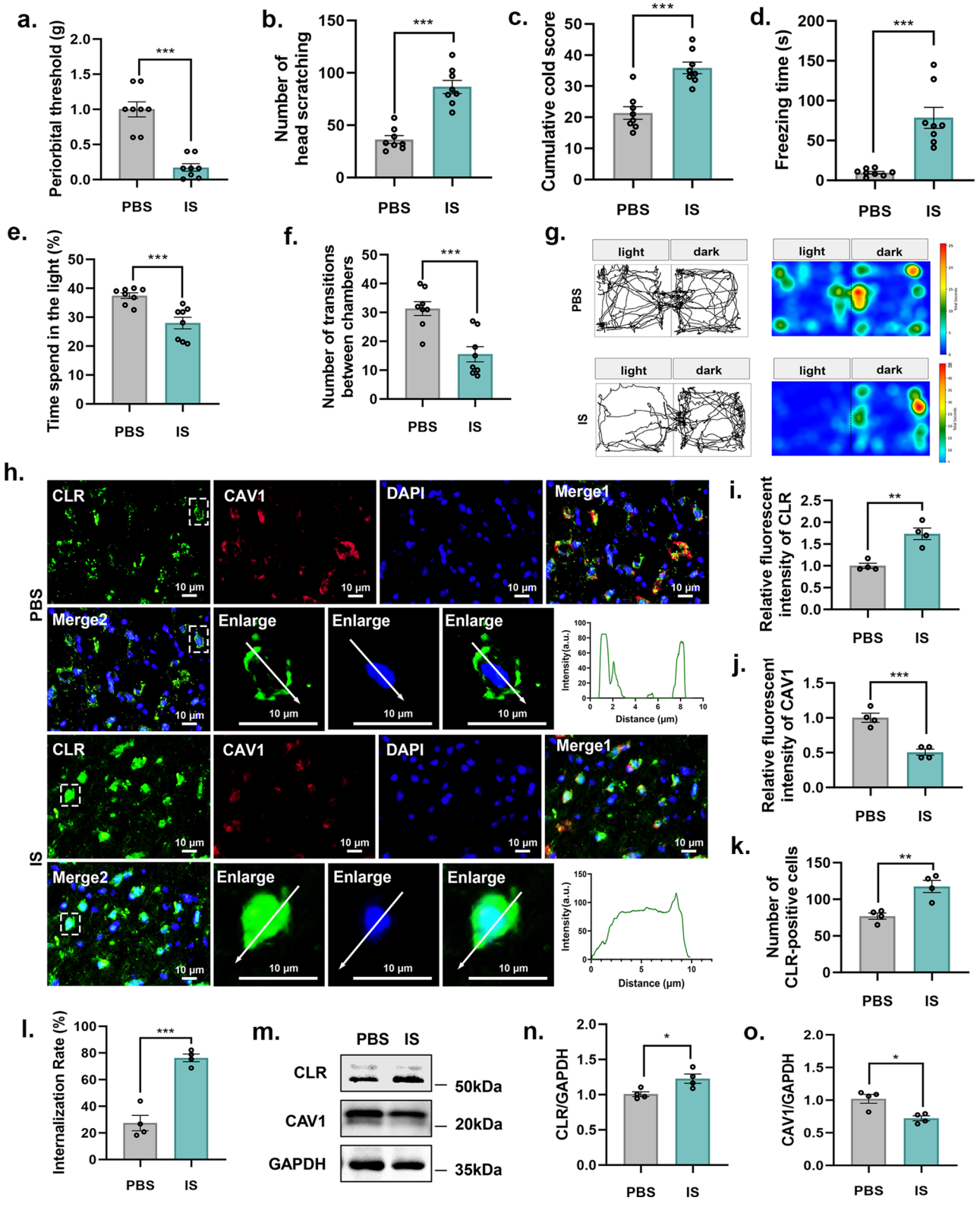

Fig. 1 (See legend on next page.)

(See figure on previous page.)

Fig. 1 Changes in CAV1/CLR expression and migraine-like behaviors in female mice after repeated dural IS stimulation. (**a**-**g**) Migraine-like behavioral results after repeated dural IS stimulation, including periorbital threshold (**a**), number of head scratching (**b**), cold pain scores (**c**), freezing time (**d**), time spent in the light (**e**), number of transitions between chambers (**f**), representative movement traces and heatmaps of the mice in the light/dark box (**g**). $n = 8$ mice per group. (**h**) Double immunofluorescence staining showed that CLR and CAV1 were co-localized in the TNC of female mice. Representative images characterizing CLR internalization are shown in an enlarged view. Line-scan plots show the fluorescence intensity profiles along the white arrows. Scale bar: 10 μm. (**i**-**j**) Quantitative analysis of CLR (**i**) and CAV1 (**j**) immunofluorescence. $n = 4$ mice per group. (**k**-**l**) Quantitative analysis of CLR-positive cells (**k**) and the ratio of internalized CLR-positive cells to total CLR-positive cells (**l**). $n = 4$ mice per group. (**m**-**o**) Representative immunoblots and quantification of CLR (**n**) and CAV1 (**o**) proteins in different groups. $n = 4$ mice per group. Mean ± SEM, unpaired Student's t-test, $^{*}p < 0.05$, $^{**}p < 0.01$ and $^{***}p < 0.001$ compared to the PBS group. *Abbreviations: CAV1: caveolin-1; CLR: calcitonin receptor-like receptor; IS, inflammatory soup; TNC: trigeminal nucleus caudalis*

periorbital mechanical thresholds, reduced pain scores, decreased head-scratching counts, shortened freezing time, and alleviated photophobia (Fig. S2a-g). No significant behavioral alterations were observed in PBS-treated control mice following BIBN4096 administration. Consistent with these behavioral findings, BIBN4096 treatment markedly suppressed IS-induced c-Fos immunoreactivity in the TNC (Fig. S2h, i), indicative of attenuated trigeminovascular neuronal activation. These findings collectively implicate CLR as a key promoter of migraine progression.

CAV1 interacts with CLR and negatively regulates its expression

To explore whether CAV1 interacts with CLR, we stimulated SH-SY5Y cells with different concentrations of CGRP (1, 3, 5, 10, 20 μM). Western blot analysis revealed that CAV1 protein levels were unchanged or even slightly increased with low-concentration CGRP stimulation (< 5 μM), but high-concentration CGRP stimulation (≥ 5 μM) resulted in a significant decrease in CAV1 protein expression (Fig. 2a, c). CLR expression remained increased in this process (Fig. 2a, b). The results indicated there might be a negative expression regulation relationship between CLR and CAV1.

Bidirectional coIP of exogenous CLR and CAV1 confirmed their robust interaction (Fig. 2d, e), further supported by their co-localization via immunofluorescence (Fig. 2f). As CAV1 is a caveolae-associated scaffolding protein critical for membrane trafficking and signaling molecule clustering [39], we focused on exploring its role in regulating CLR.

SH-SY5Y cells were transfected with CAV1-FLAG plasmid to increase CAV1 expression, while an empty vector plasmid was transfected to serve as a negative control. The results suggested that CLR protein level was reduced in response to CAV1 overexpression ($p < 0.05$, Fig. 2g, h). CoIP experiments using TNC tissue from IS-treated mice revealed enhanced CAV1-CLR interaction relative to PBS controls (Fig. 2i, j). These findings suggest that CAV1 and CLR might repress each other's expression through direct protein-protein interactions. The expression of CAV1 was decreased in migraine mice, and the decreased CAV1 likely upregulates CLR protein levels through a process involving the CLR-interacting domain of CAV1. Conversely, CAV1 overexpression suppresses CLR expression.

IS enhanced CLR internalization via caveolin-dependent endocytosis

Ligand-induced receptor endocytosis remains a hallmark feature of GPCR activation and downstream signal transduction [40]. Building on our observation of IS-induced CLR internalization in the TNC (Fig. 1h, l), we further examined and quantified CLR trafficking in the trigeminal ganglion. Results revealed that IS-treated mice exhibited higher CLR-positive cell counts and internalization rates than controls (Fig. 3a-c). Consistent with this, western blot analysis showed a reduced membrane-to-cytosol ratio of CLR in the IS group (approximately 78%) compared to the PBS group (approximately 82%, Fig. 3d-e). Given that caveolae and CAV1 participate in GPCR endocytosis [41], we hypothesized that CAV1 regulates CLR subcellular trafficking. In SH-SY5Y cells, immunofluorescence staining showed that CAV1 plasmid transfection significantly enhanced CLR internalization, characterized by a reduced ratio of membrane-localized to cytoplasmic CLR (Fig. 3f, g). Western blot analysis further demonstrated that CAV1 overexpression reduced CLR protein levels not only in the membrane fraction but also in the cytoplasmic fraction, accompanied by a pronounced decrease in the membrane-to-cytoplasmic ratio of CLR (Fig. S3a-d). These data collectively suggest that CAV1 promotes CLR internalization and subsequent downregulation.

To determine the endocytic pathway for CLR internalization, we applied various endocytosis inhibitors to SH-SY5Y cells. Cellular uptake assay investigated the impact of different inhibitors on CLR cellular internalization efficiency. Results showed that nystatin (inhibits caveolin-mediated endocytosis) significantly prevented CLR internalization after 1 h of CGRP stimulation ($p < 0.001$). In contrast, sucrose (inhibits clathrin-mediated endocytosis), amiloride (inhibits macropinocytosis), and chloroquine (inhibits endosomal acidification and membrane fusion) had little or no effect on CLR internalization [42] (Fig. 3h-i). These findings establish caveolae as the

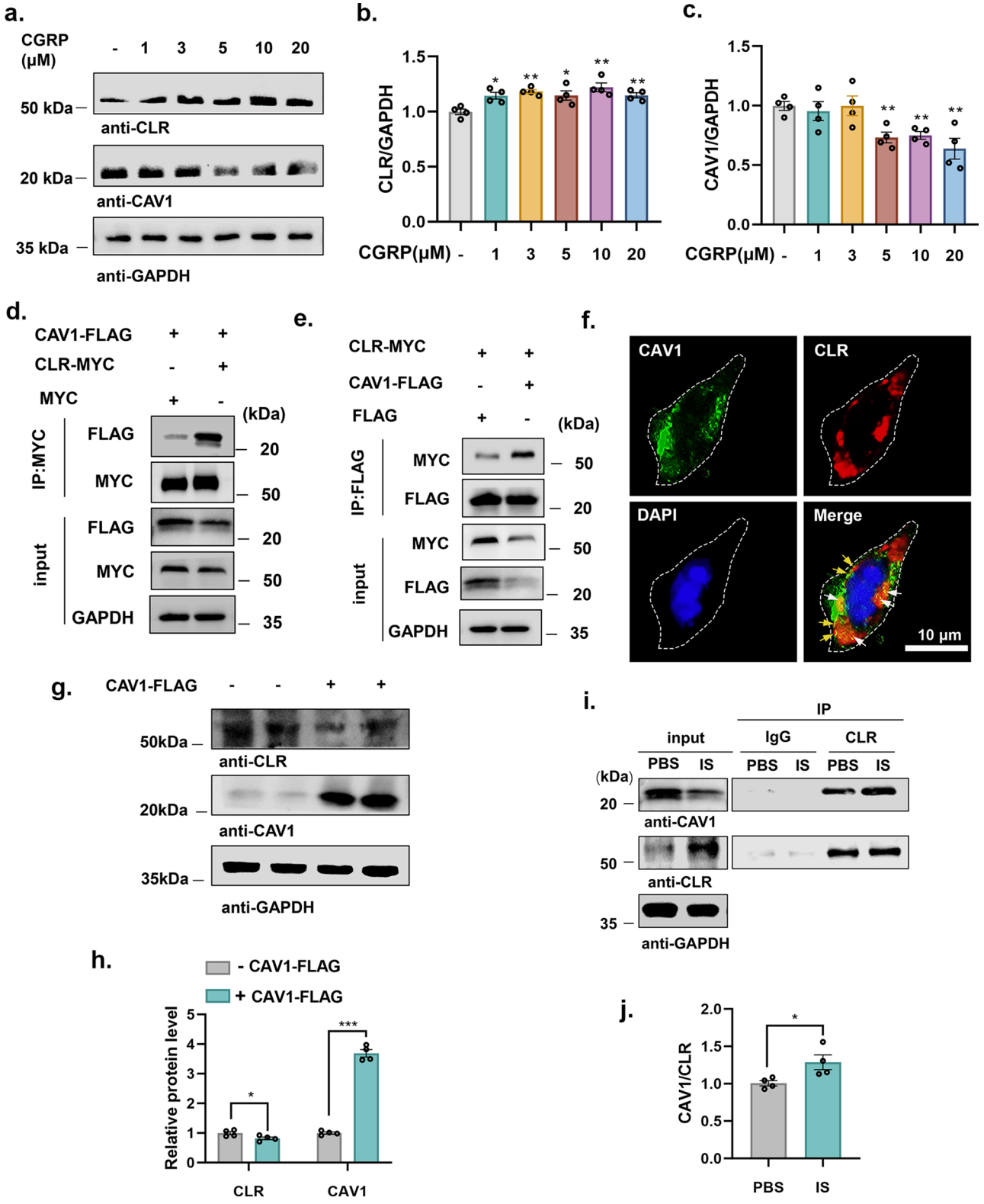

Fig. 2 (See legend on next page.)

(See figure on previous page.)

Fig. 2 The interaction between CAV1 and CLR. (**a-c**) Effects of CGRP on CLR (**b**) and CAV1 (**c**) proteins in SH-SY5Y cells. $n = 4$ independent experiments. Mean ± SEM, One-way ANOVA, *$p < 0.05$, and **$p < 0.01$ compared to the control without CGRP stimulation. (**d-e**) CoIP of CLR with CAV1 in SH-SY5Y cells. (**f**) Immunofluorescence co-localization of CAV1 and CLR in SH-SY5Y cells. Scale bar: 10 μm. Yellow arrowheads indicate membrane-associated co-localized puncta, while white arrowheads mark cytosolic colocalization sites. (**g-h**) Effects of CAV1 overexpression on CLR protein levels assessed by western blot in SH-SY5Y cells. $n = 4$ independent experiments. Mean ± SEM, unpaired Student's t-test, *$p < 0.05$, ***$p < 0.001$ compared to the negative control. (**i-j**) Representative coIP immunoblots of CLR with CAV1 and quantification in the TNC of female mice. $n = 4$ independent experiments. Mean ± SEM, unpaired Student's t-test, *$p < 0.05$ compared to the negative control. *Abbreviations: CAV1: caveolin-1; CLR: calcitonin receptor-like receptor; CGRP: calcitonin gene-related peptide; coIP: co-immunoprecipitated*

dominant pathway for CLR internalization and underscore CAV1's regulatory role in migraine mechanisms.

CAV1 regulated neuronal ERK/CREB pathway activation and microglial inflammation through neuron-microglia interaction

Previous studies have implicated the involvement of ERK/CREB pathway activation, microglial activation, and inflammation in migraine pathogenesis [35, 43], all of which are linked to CAV1 [44]. We investigated CAV1's role in modulating these pathways. Western blot analysis revealed increased phosphorylation of ERK1/2 ($p < 0.001$) and CREB ($p < 0.05$) in the TNC of female mice following repeated IS stimulation (Fig. 4a-b). IS-treated mice also exhibited pronounced microgliosis in TNC, characterized by elevated IBA1 immunoreactivity (a microglial marker; Fig. 4c, d). Morphological analysis showed an enlarged cell body with shorter and thicker microglia in the IS group, suggesting enhanced activation (Fig. 4e). Additionally, IS stimulation triggered neuroinflammation, as demonstrated by elevated TNFα ($p < 0.001$) and IL-1β ($p < 0.01$) protein levels (Fig. 4f-g). To elucidate the role of CAV1, we overexpressed CAV1 in SH-SY5Y cells using lentiviral transduction. CAV1 overexpression significantly suppressed phosphorylated ERK ($p < 0.001$) and CREB ($p < 0.01$; Fig. 4h, i), indicating inhibition of the ERK/CREB pathway. To investigate the impact of neuronal CAV1 on microglial inflammation, BV2 cells were treated with conditioned medium from CAV1-overexpressing SH-SY5Y cells for 24 h (Fig. 4j). Results showed that neuronal CAV1 overexpression significantly reduced TNFα ($p < 0.01$) and IL-1β ($p < 0.001$) levels in microglia (Fig. 4k, l), demonstrating its ability to attenuate microglial-mediated neuroinflammation.

CAV1 knockdown triggered migraine-like behavioral traits in female mice

To further clarify the regulatory role of CAV1 in migraine pathogenesis, we microinjected siRNA targeted CAV1 into the TNC of female mice. First, we screened three CAV1 siRNAs (CAV1-siRNA1/2/3) in BV2 cells using negative control (NC) siRNA as a comparator. identified CAV1-siRNA2 as the most effective, achieving ~65% CAV1 knockdown and concurrently increasing CLR expression by ~120% (Fig. 5a, b). CAV1-siRNA2 was therefore selected for subsequent in vivo experiments. The experimental design is shown in Fig. 5c.

Behavioral assays revealed that CAV1 knockdown mimicked IS stimulation, eliciting decreased periorbital and cold withdrawal thresholds, increased spontaneous pain-related behaviors (head-scratching, freezing), and increased photophobia compared to NC controls (Fig. 5d-j). The immunofluorescence of c-Fos in the TNC confirmed that CAV1 knockdown induced activation of the trigeminovascular system in female mice (Fig. S2a, b). Compared with mice in the NC group, mice with CAV1 knockdown exhibited increased release of CGRP (Fig. S2c, d). Molecular analyses demonstrated increased phosphorylation of ERK ($p < 0.05$) and CREB ($p < 0.05$), elevated CLR protein levels ($p < 0.05$), and upregulated TNFα ($p < 0.01$) and IL-1β ($p < 0.05$) in the TNC of CAV1-knockdown mice versus NC mice (Fig. 5k, l). Furthermore, immunofluorescence and morphological analyses confirmed microglial aggregation and activation in TNC tissue following CAV1 knockdown (Fig. 5m–o). Collectively, these results demonstrate that CAV1 deficiency alone recapitulates migraine-like behavioral and neuroinflammatory phenotypes, underscoring CAV1 as a pivotal therapeutic target in migraine.

MβCD suppressed ERK/CREB activation and inflammatory factors production in vitro

The above studies suggested that CAV1 may regulate the downstream signaling involved in migraine by mediating CLR internalization. To explore this further, we used MβCD, a typical lipid raft-mediated endocytosis inhibitor, to block CAV1 function [31]. First, we administered MβCD (5 mM) and CGRP (1 μM) individually or in combination to SH-SY5Y cells. WB analysis was performed to assess the effects on CLR and ERK/CREB signaling pathways. The sole application of CGRP significantly stimulated the phosphorylation of ERK ($p < 0.001$) and CREB ($p < 0.001$), while MβCD had the opposite effect (Fig. 6a-c). Combined treatment with MβCD attenuated CGRP-induced ERK/CREB pathway activation (Fig. 6a-c). MβCD treatment did not decrease or even slightly increase CLR protein levels (Fig. 6a, d). MβCD alone depleted CAV1 ($p < 0.001$), and CAV1 levels were further reduced by combined CGRP administration (Fig. 6a, e). Next, we examined the effects of CGRP and MβCD on the release of inflammatory factors. MβCD significantly

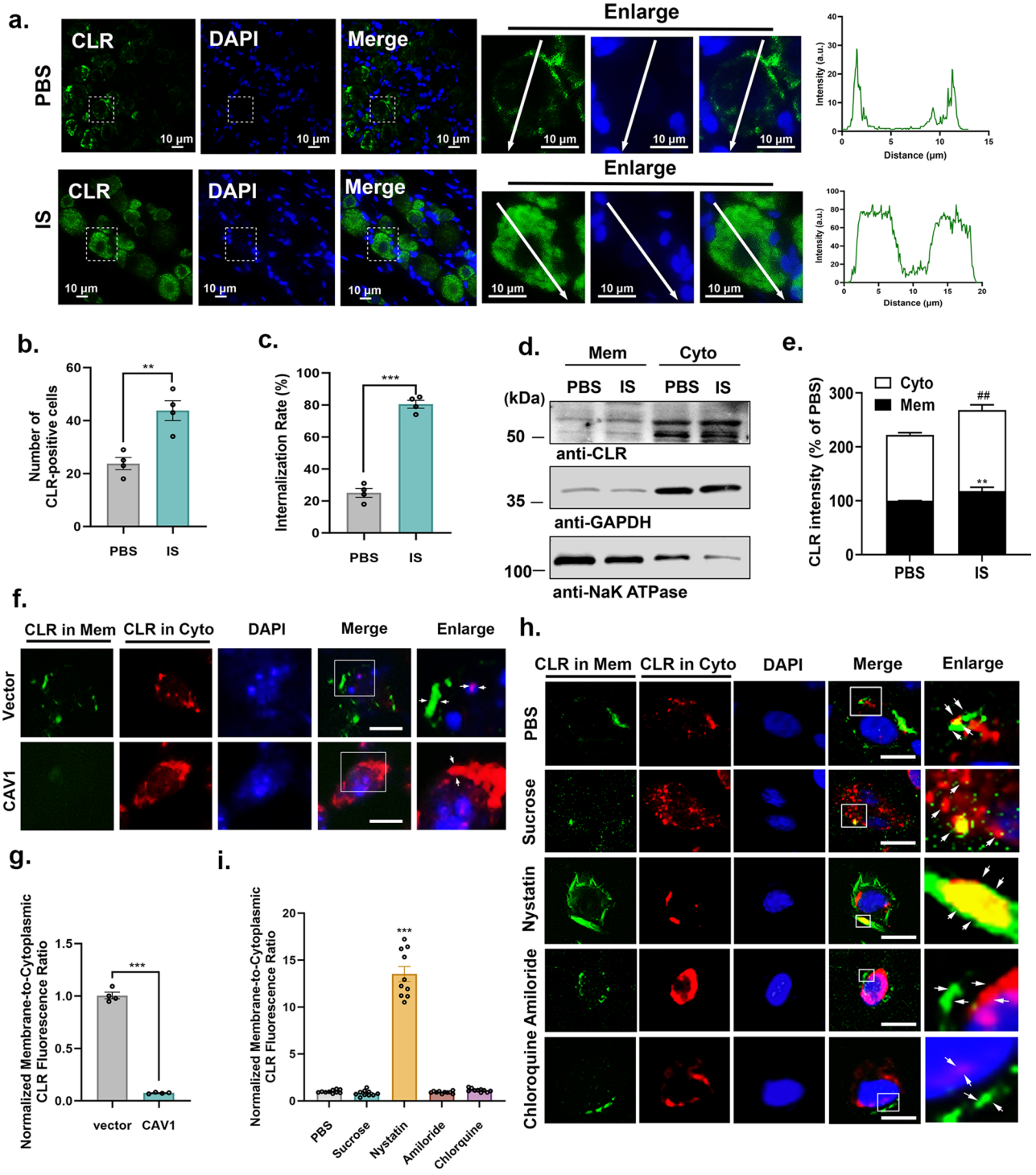

Fig. 3 CLR internalization and endocytic pathway. (**a**) Representative immunofluorescence staining images showed that IS-induced CLR internalization in the trigeminal ganglion. Insets show a higher magnification view. Line-scan plots show the fluorescence intensity profiles along the white arrows. Scale bar: 10 μm. $n = 4$ mice per group. (**b**-**c**) Quantitative analysis of CLR-positive cells (**b**) and the ratio of internalized CLR-positive cells to total CLR-positive cells (**c**). $n = 4$ mice per group. (**d**-**e**) Representative immunoblots and quantification of CLR in the cytosol and the cytomembrane after repeated dural IS stimulation. $n = 4$ mice per group. Mean ± SEM, unpaired Student's t-test, $^{**}p < 0.01$ compared to the cytomembrane protein levels in the PBS group, $^{\#\#}p < 0.01$ compared to the cytosol protein levels in the PBS group. (**f**) Representative immunofluorescence images of CLR protein in the cytomembrane (green) and the cytosol (red) after CAV1 overexpressing. Scale bar, 10 μm. (**g**) Quantification of the ratio of membrane to cytoplasmic-cell fluorescence. $n = 4$ cells per group. (**h**) Representative immunofluorescence images and quantification of CLR protein in the cytomembrane (green) and the cytosol (red) after applying endocytosis inhibitors. Scale bar, 10 μm. (**i**) Quantification of the ratio of membrane to cytoplasmic-cell fluorescence. $n = 4$ cells per group. *Abbreviations: CLR: calcitonin receptor-like receptor; RAMP1: receptor activity modifying protein 1; IS, inflammatory soup; Mem: cytomembrane; Cyto: cytosol; PBS: Phosphate buffer saline*

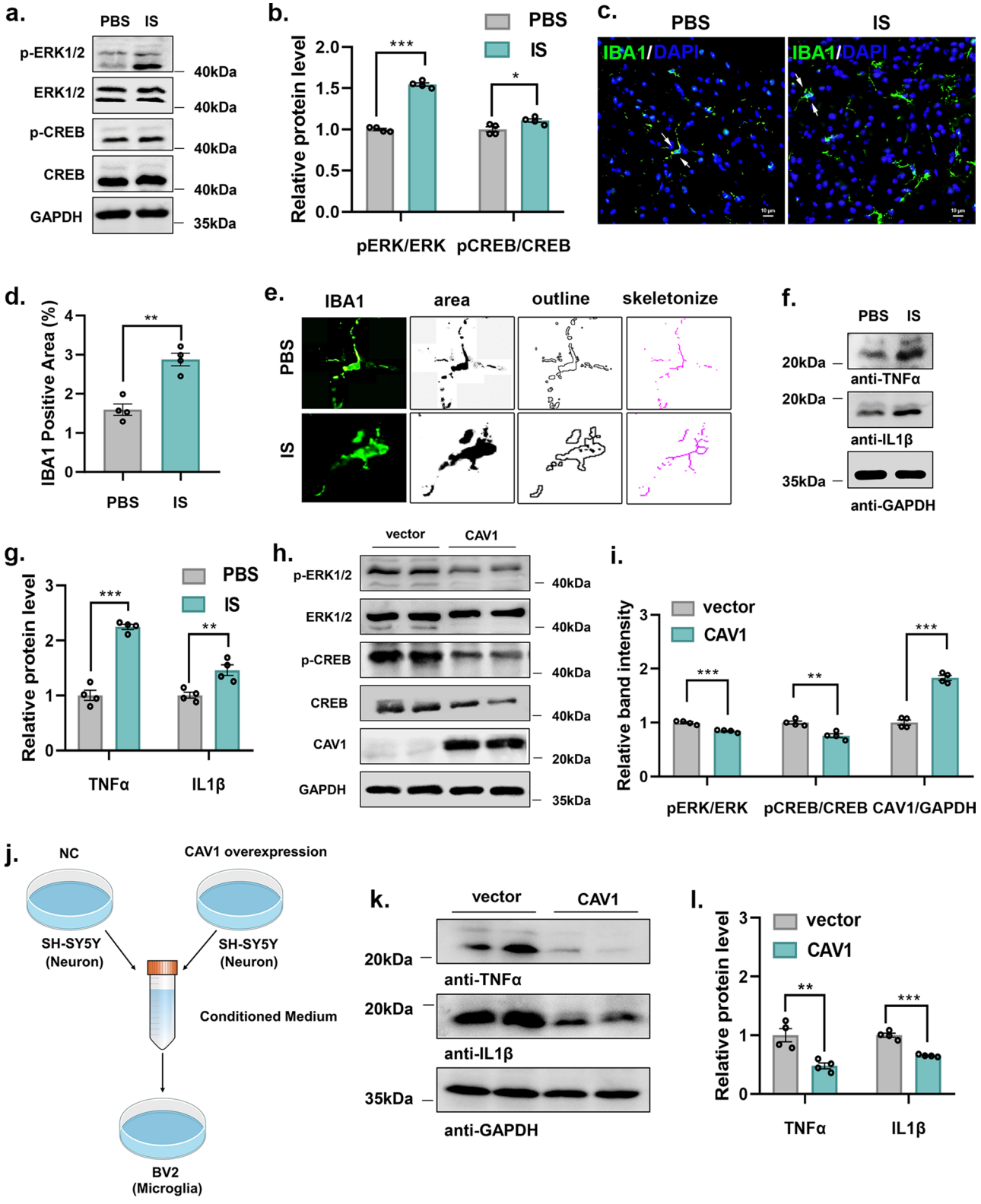

Fig. 4 (See legend on next page.)

(See figure on previous page.)

Fig. 4 CAV1 regulated ERK/CREB pathway and microglia activation. (**a**-**b**) Representative immunoblots and quantification of ERK/CREB pathway in the TNC. $n = 4$ mice per group. Mean ± SEM, unpaired Student's t-test, $^{*}p < 0.05$, $^{***}p < 0.001$ compared to the PBS group. (**c**-**d**) Representative immunofluorescence images and quantification of IBA1 in the TNC. Scale bar: 10 μm. $n = 4$ mice per group. Mean ± SEM, unpaired Student's t-test, $^{**}p < 0.01$ compared to the PBS group. (**e**) Typical microglial morphology in the TNC after repeated dural IS stimulation. (**f**-**g**) Representative immunoblot images and quantification of TNFα and IL-1β in the TNC. $n = 4$ mice per group. Mean ± SEM, unpaired Student's t-test, $^{**}p < 0.01$, $^{***}p < 0.001$ compared to the PBS group. (**h**-**i**) Effects of CAV1 overexpression on ERK/CREB pathway assessed by western blot in SH-SY5Y cells. $n = 4$ independent experiments. Mean ± SEM, unpaired Student's t-test, $^{**}p < 0.01$, $^{***}p < 0.001$ compared to the vector group. (**j**) Diagram of culture conditions. (**k**-**l**) Effects of CAV1 overexpression in SH-SY5Y cells on the release of TNFα and IL-1β from BV2 cells, as assessed by western blot. $n = 4$ independent experiments. Mean ± SEM, unpaired Student's t-test, $^{**}p < 0.01$, $^{***}p < 0.001$ compared to vector. *Abbreviations: CAV1: caveolin-1; TNC: trigeminal nucleus caudalis*

reduced the expression of IL-1β ($p < 0.001$) induced by CGRP stimulation (Fig. 6f-h). The level of TNFα was declined by the treatment of MβCD alone or in combination with CGRP. These results indicated that MβCD suppresses ERK/CREB activation and inflammatory factor production in vitro, implicating its potential role in modulating migraine-related signaling pathways.

MβCD alleviated hyperalgesia and neuroinflammation in female migraine mice

To verify the role of MβCD in vivo, MβCD was further injected intranasally in the mice after PBS or IS stimulations (Fig. 7a). Compared to the IS-VEH group, the IS-MβCD group exhibited reduced periorbital mechanical ($p < 0.001$) and cold pain thresholds ($p < 0.01$), alongside increased spontaneous pain behaviors (head-scratching, $p < 0.01$; freezing time, $p < 0.05$) and photophobia ($p < 0.05$; Fig. 7b–h). MβCD alone had no significant effect on migraine-like behaviors in female mice. MβCD treatment significantly reduced IS-induced c-Fos ($p < 0.01$) and CGRP immunoreactivity ($p < 0.001$), whereas MβCD alone had minimal effects on these markers (Fig. S1a–d). In addition, MβCD alone downregulated inflammatory factor (TNFα, $p < 0.001$; IL-1β, $p < 0.05$) while upregulated CLR ($p < 0.05$) protein levels in female mice compared with the PBS-VEH group (Fig. 7i-j). MβCD treatment after IS stimulation decreased the activation of the ERK/CREB pathway and expression of TNFα ($p < 0.001$) and IL-1β ($p < 0.05$) but did not reduce a decrease in CLR ($p = 0.694$) expression (Fig. 7i-j). CLR internalization in the mouse TNC was also examined. There was no statistically significant difference in the cytoplasm CLR expression in the IS-MβCD group compared to the IS-VEH group. At the same time, MβCD increased the cell surface CLR after IS infusions (Fig. 7k-l). The results indicated that the ratio of CLR entry into the cytoplasm in the IS-MβCD group was decreased compared to the IS-VEH group. Immunofluorescence showed that MβCD treatment reduced the number and activation of microglia in the TNC of female mice induced by IS stimulations ($p < 0.001$, Fig. 7m-n). Taken together, MβCD inhibited CLR internalization, suppressed ERK/CREB pathway activation, and reduced microglia-mediated inflammation factors release. These findings suggested that blocking the CAV1-CLR trafficking axis with MβCD may be an effective strategy for migraine treatment.

CAV1 overexpression attenuated migraine-like behaviors via the CLR/ERK/CREB signaling and microglia activation in female migraine mice

Finally, we performed functional rescued for CAV1 overexpression to examine the therapeutic potential of CAV1 in vivo. Female mice were microinjected with lentivirus overexpressing CAV1 prior to IS stimulation (Fig. 8a). Behavioral and related molecular indicators were examined in mice after modeling completion. Compared to the LV-NC + IS group, mice in the LV-CAV1 + IS group exhibited increased periorbital and cold pain thresholds, decreased spontaneous pain behaviors, and reduced photophobia (Fig. 8b-h), indicating that CAV1 alleviated migraine-like behaviors induced by repeated IS stimulation. CAV1 overexpression also rescued IS-induced increases in c-Fos ($p < 0.01$) and CGRP ($p < 0.05$) expression (Fig. S4a-d). CAV1 overexpression downregulated the phosphorylation of ERK ($p < 0.05$) and CREB ($p < 0.05$), and reduced CLR protein levels ($p < 0.001$) and inflammatory factors expression (TNFα, $p < 0.01$; IL-1β, $p < 0.05$) in the TNC of female mice (Fig. 8i, j). Morphological changes and decreased IBA1 immunoreactivity in the LV-CAV1 + IS group suggested that CAV1 attenuated IS-induced microglial activation and gliosis (Fig. 8k, l). These findings showed that combined gene therapy targeting CAV1 could be an effective treatment strategy for migraine.

Discussion

Our findings establish CAV1 in the TNC of female mice as a key regulator of IS-induced migraine-like pathology. CAV1 acts as a molecular checkpoint, integrating CLR signaling with neuroinflammatory processes and offering mechanistic insights into migraine pathophysiology. These results highlight CAV1-targeted interventions as potential therapeutic strategies for migraine.

In migraine pathogenesis, IS stimulation elevated CGRP levels (Fig. S1c-d), leading to CLR activation and subsequent receptor internalization (Figs. 1h and 3a). CAV1 modulated caveolae-mediated CLR endocytosis through physical interaction and CLR expression regulation (Fig. 2d-i). During migraine progression, decreased

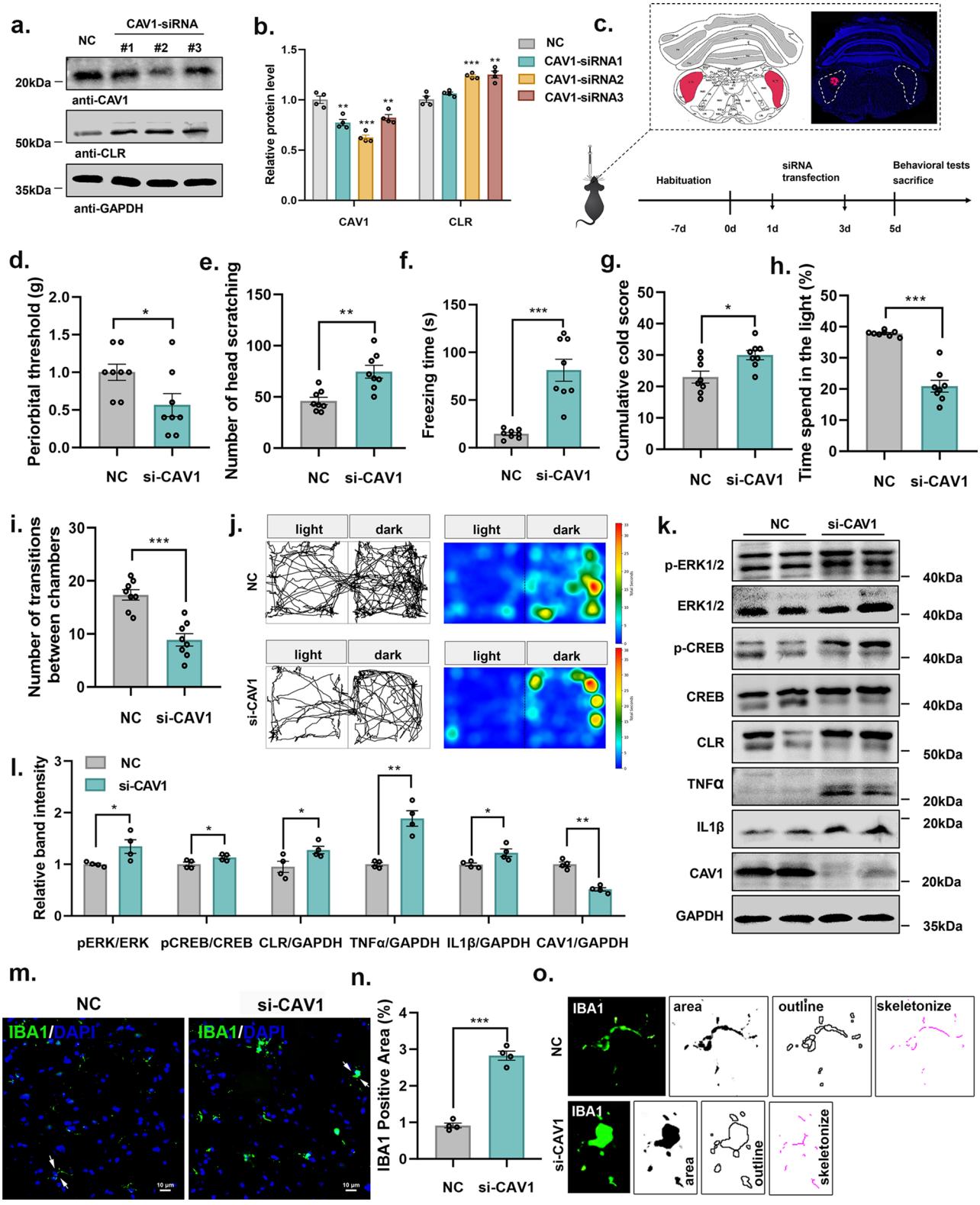

Fig. 5 (See legend on next page.)

(See figure on previous page.)

Fig. 5 CAV1 knockdown induced migraine-like symptoms by regulating the CLR/ERK/CREB pathway and microglia activation in vivo. (**a**-**b**) Representative immunoblots and quantification of CAV1/CLR after siRNA treatment in BV2 cells. $n = 4$ independent experiments. Mean ± SEM, unpaired Student's t-test, $^{**}p < 0.01$, $^{***}p < 0.001$ compared to the negative control. (**c**) Experimental flow chart and schematic of the siRNA microinjection site. (**d**-**j**) Migraine-like behavioral results after CAV1-siRNA microinjection, including periorbital threshold (**d**), number of head scratching (**e**), freezing time (**f**), cold pain scores (**g**), time spent in the light (**h**), number of transitions between chambers (**i**), representative movement traces and heatmaps of the mice in the light/dark box (j). $n = 8$ mice per group. (**k**-**l**) Representative immunoblots and quantitative analysis of CLR, ERK/CREB signaling, and TNFα/IL-1β protein levels in the TNC after CAV1-siRNA microinjection. $n = 4$ mice per group. (**m**-**n**) Representative immunofluorescence images and quantification of IBA1 in the TNC after CAV1-siRNA microinjection. Scale bar: 10 μm. $n = 4$ mice per group. (**o**) Typical microglial morphology in the TNC after CAV1-siRNA microinjection. Mean ± SEM, unpaired Student's t-test, $^{*}p < 0.05$, $^{**}p < 0.01$ and $^{***}p < 0.001$ compared to the NC group. *Abbreviations: CAV1: caveolin-1; CLR: calcitonin receptor-like receptor; TNC: trigeminal nucleus caudalis*

CAV1 expression was observed (Fig. 1m, o), concurrent with CLR internalization, ERK/CREB pathway activation, microglial priming, and pro-inflammatory factors release (Fig. 4a-g). These events correlated with neuronal sensitization, accompanied by nociceptive hypersensitivity and photophobia. TNC-specific CAV1 knockdown recapitulated key pathological features. CAV1 knockdown upregulated CLR expression, amplified ERK/CREB signaling, and exacerbated neuroinflammation (Fig. 5). Pharmacological caveolae disruption using MβCD reduced CLR internalization, ERK/CREB activation, and cytokine production in IS models, consequently attenuating migraine symptoms (Fig. 7). Therapeutic overexpression of CAV1 shifted CLR fate by promoting robust receptor internalization (Fig. 3f-g; Fig. S3a-d), redirecting internalized CLR to degradation rather than recycling. In this process, CGRP-bound CLR underwent co-degradation within caveolae-derived vesicles, reducing extracellular CGRP (Fig. S6c-d). This CAV1-mediated disruption of CGRP/CLR signaling, along with the suppression of ERK/CREB activation and neuroinflammation (Fig. 8i-k), ultimately reversed IS-induced migraine-like behaviors (Fig. 9).

In our study, CAV1 knockdown increased CGRP expression, hinting at complex interactions between CAV1, CGRP/CLR signaling, and the trigeminovascular system. CAV1 depletion upregulates CLR, sustaining its activation. This triggers trigeminovascular activation and further CGRP release, thereby amplifying nociceptive transmission [45, 46]. Moreover, CAV1 knockdown-induced microglial activation releases pro-inflammatory cytokines such as TNFα and IL-1β, which can further stimulate neuronal CGRP production [47, 48], intensifying this cycle. Conversely, CAV1 overexpression and MβCD treatment can block CLR signaling and suppress microglial-mediated inflammatory amplification, disrupting this pathological cascade. However, further research is needed to understand the intricate mechanisms underlying these interactions fully.

CLR internalization activates multiple intracellular signaling pathways to amplify pain signals [36, 49, 50]. Among these pathways, the ERK/CREB pathway received significant attention and has been extensively studied [50]. For instance, in one study related to pain, CGRP was found to stimulate CLR endocytosis and activate PKC in the cytosol and ERK in the cytosol and nucleus. Inhibiting CLR endocytosis prevented the activation of cytosolic PKC and nuclear ERK [49]. Zhou et al. further demonstrated that blocking CGRP/CLR signaling downregulated the expression levels of p-ERK and p-CREB by using a CGRP receptor antagonist in a chronic migraine rat model [36]. These findings confirm that CGRP/CLR signaling directly triggers ERK activation. Therefore, we focused on upstream regulatory mechanisms rather than revalidating this established pathway. Here, we identify CAV1 as a pivotal modulator of the CLR/ERK/CREB pathway in migraine pathophysiology. By employing CAV1 knockdown and overexpression, we demonstrated that CAV1 negatively regulates ERK/CREB signaling, dampening CLR-mediated nociceptive amplification and migraine-like behaviors (Figs. 5d-l and 8b-j). The effect of CAV1 on the ERK/CREB pathway in migraine may be direct or indirect, potentially mediated through its interaction with CLR. The role of ERK/CREB in CAV1-mediated migraine pathogenesis and their interaction with CAV1-CLR signaling requires further study.

As a key structural component of caveolae, CAV1 orchestrates membrane and receptor dynamics [17]. Following GPCR activation, CAV1 undergoes internalization, phosphorylation, and ubiquitination [51]. Under physiological conditions, CAV1 maintains homeostasis via recycling mechanisms [17]. However, excessive CGRP exposure may induce cellular stress. Pathological conditions disrupt this balance, inducing caveolae disassembly and CAV1 degradation [52]. Future studies are needed to elucidate the mechanisms underlying CGRP-induced CAV1 degradation. Our study found decreased CAV1 expression in the TNC of IS-induced migraine (Fig. 1m, o). Whether this reduction is attributable to pathological CGRP stimulation also requires further investigation.

There are two classical endocytosis pathways: clathrin-dependent and clathrin-independent [53]. Using different endocytic inhibitors, we found that caveolae and caveolin-1 mediated CLR internalization induced by CGRP stimulation in SH-SY5Y cells (Fig. 3h, i). Similar to our observations, another study by Tang et al. concluded that CLR internalization is mediated by the caveolae-dependent pathway on VSMC [54]. However, many other studies presented clathrin-mediated CLR internalization [9,

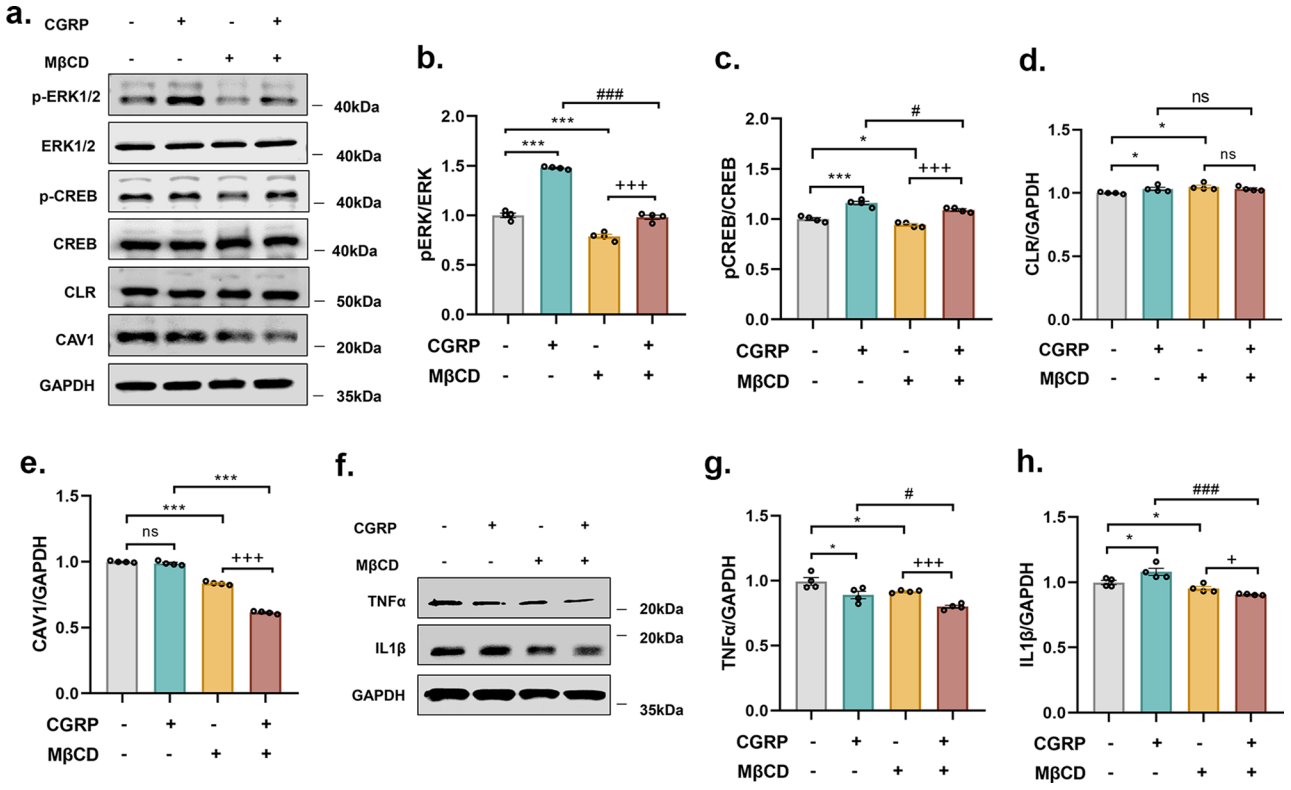

Fig. 6 MβCD attenuated ERK/CREB signaling and inflammation in vitro. (**a**-**e**) Effects of MβCD on ERK/CREB activation and CAV1/ CLR with or without CGRP stimulation (1 μM) in SH-SY5Y cells were analyzed by western blotting. $n = 4$ independent experiments. Mean ± SEM, One-way ANOVA, $^{*}p < 0.05$, $^{**}p < 0.01$, $^{***}p < 0.001$ vs. untreated control; $^{+++}p < 0.001$ vs. MβCD alone; $^{\#\#}p < 0.01$, $^{\#\#\#}p < 0.001$ vs. CGRP alone. (**f**-**h**) Effects of MβCD on TNFα and IL1β protein levels with or without CGRP stimulation (1 μM) in BV2 cells were analyzed by western blotting. $n = 4$ independent experiments. Mean ± SEM, One-way ANOVA, $^{*}p < 0.05$ compared to the control without stimulation, $^{+}p < 0.05$ compared to the control with MβCD stimulation alone. $^{\#}p < 0.05$, and $^{\#\#\#}p < 0.001$ compared to the control with CGRP stimulation. *Abbreviations: MβCD: methyl-β-cyclodextrin; CAV1: caveolin-1; CLR: calcitonin receptor-like receptor; ns: not significant*

49, 55]. The discrepancy is likely attributable to the fact that these studies only used inhibitors of clathrin-mediated endocytosis, but not caveolae-mediated inhibitors. CAV1 may bind to CLR, promoting its lysosomal degradation and inhibiting CLR signaling. This mechanism is also observed in other CAV1-mediated receptor pathways. For example, CAV1 inhibits TGF-β signaling by mediating the lysosomal degradation of TGF-β receptors through caveolae/raft-dependent endocytosis [56]. Specifically, CAV1 interacts with TGF-β receptors, preventing their interaction with SMAD proteins and downstream signaling. Additionally, caveolae and membrane rafts facilitate the recruitment of ubiquitin ligases, which promote the ubiquitination and degradation of CAV1 and TGF-β receptors. In this context, CAV1 recruits ubiquitinated TGF-β receptors in the plasma membrane and aids their transport to lysosomes, thereby inhibiting TGF-β signaling.

To further test the role of CLR internalization in migraine, we used MβCD to block the caveolin-dependent internalization. MβCD is a well-known cholesterol-depleting agent that selectively extracts cholesterol from the plasma membrane bilayer, thereby disrupting lipid raft integrity without perturbing other membrane components [57, 58]. Importantly, MβCD primarily exerts its effects by inhibiting caveolae-dependent internalization rather than directly modulating the expression of CAV1. The impact of MβCD on CAV1 expression is dynamic. Nascimento et al. reported that CAV1 expression decreased at 6 h but increased at 24 h following MβCD-induced cholesterol depletion [57]. In our experimental paradigm, tissues were collected shortly after behavioral assessments (within 24 h of the final MβCD dose), potentially capturing the early phase of CAV1 downregulation. However, this transient reduction in CAV1 expression does not negate its functional inhibition. CAV1 is predominantly localized in the plasma membrane, whereas ERK and CREB are primarily found in the cytoplasm and nucleus [36, 51]. CAV1 and CLR rely on caveolae-mediated internalization to initiate downstream signaling. MβCD prevents their internalization, thereby disrupting CLR/CAV1 trafficking to intracellular compartments required for ERK/CREB pathway activation. Consequently, even if the expression of CAV1

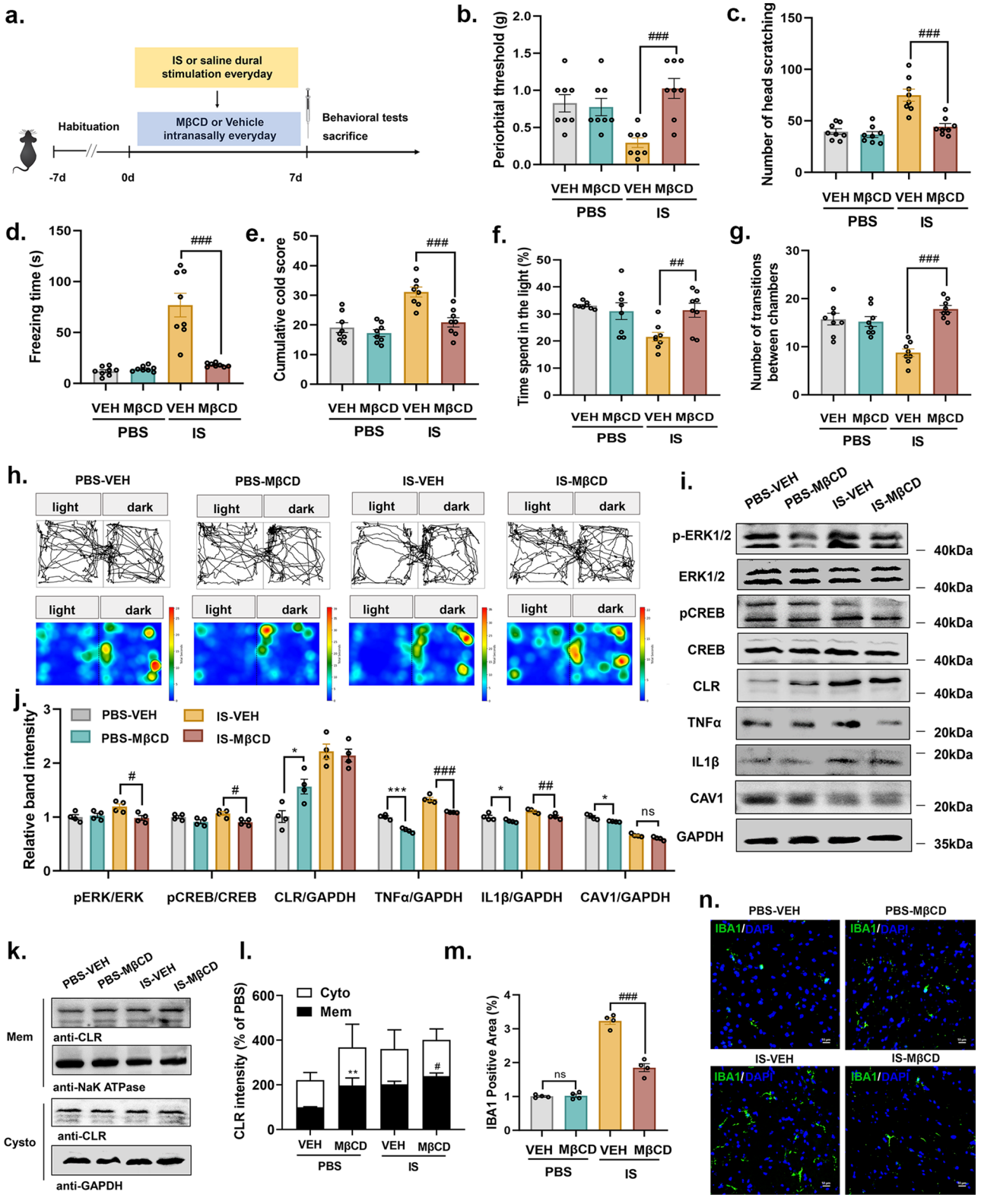

Fig. 7 (See legend on next page.)

(See figure on previous page.)

Fig. 7 Evaluation of MβCD effect in female mice. (**a**) Flow chart of experimental procedure in vivo. (**b**-**h**) Migraine-like behavioral results after MβCD infusion on IS-induced migraine mice, including periorbital threshold (**b**), number of head scratching (**c**), freezing time (**d**), cold pain scores (**e**), time spent in the light (**f**), number of transitions between chambers (**g**), representative movement traces and heatmaps of the mice in the light/dark box (**h**). $n = 8$ mice per group. Mean ± SEM, One-way ANOVA, $^{\#\#}p < 0.01$, $^{\#\#\#}p < 0.001$ compared with IS-VEH group. (**i**-**j**) Representative immunoblots and quantification of CLR/ERK/CREB signaling and TNFα/IL1β in the TNC after MβCD infusion on IS-induced migraine mice. $n = 4$ mice per group. Mean ± SEM, One-way ANOVA, $^{*}p < 0.05$, $^{*}p < 0.001$ as compared with PBS-VEH group, $^{\#}p < 0.05$, $^{\#\#}p < 0.01$ and $^{\#\#\#}p < 0.001$ compared with IS-VEH group. (**k**-**l**) Representative immunoblots and quantification of CLR in the cytosol and the cytomembrane after MβCD infusion on IS-induced migraine mice. $n = 4$ mice per group. Mean ± SEM, One-way ANOVA, $^{**}p < 0.01$ compared to the cytomembrane protein levels in the PBS-VEH group, $^{\#}p < 0.05$ compared to the cytomembrane protein levels in the IS-VEH group. (**m**-**n**) Representative immunofluorescence images and quantification of IBA1 in the TNC after MβCD infusion on IS-induced migraine mice. Scale bar: 10 μm. $n = 4$ mice per group. Mean ± SEM, $^{\#\#\#}p < 0.001$ as compared with IS-VEH group. *Abbreviations: MβCD: methyl-β-cyclodextrin; CAV1: caveolin-1; CLR: calcitonin receptor-like receptor; TNC: trigeminal nucleus caudalis; ns: not significant*

were decreased, its inability to internalize renders it functionally inert, effectively decoupling the CAV1/CLR axis from downstream ERK/CREB signaling. This explains the marked attenuation of neuroinflammatory markers (e.g., TNFα, IL-1β) and migraine-like behaviors observed in our model (Fig. 7). Thus, while MβCD's acute effects on CAV1 expression may appear paradoxical, it exerted an overall alleviating effect on migraine symptoms.

Microglia have been regarded as the immune cells in the nervous system [59]. In disease states, microglia proliferate, migrate, and accumulate in damaged areas, participating in inflammatory responses and tissue repair [60]. The morphology of microglia is highly plastic. Activated microglia have enlarged cytosol, shorter protrusions, and rounded or rod-shaped cell morphology [61]. Targeting CAV1 can effectively alleviate IS-induced microglia proliferation and activation in female mice TNC (Figs. 7m-m and 8k-l). CAV1 overexpression caused microglia protrusions to become significantly longer (Fig. 8k). Niesman et al. also showed that microgliosis is increased in the brains of young CAV-1 knock-out (KO) mice and that CAV1 modulates microglia morphology [23]. Notably, CAV1 has been shown to promote neuroinflammation in other neurological disorders, such as traumatic brain injury, potentially through the direct activation of microglia [62]. Our study focused on the indirect effects of CAV1 on inflammatory factors released by microglia (BV2) and their subsequent impact on neurons (SH-SY5Y). The effects of CAV1 on microglia and neuroinflammation are determined by the cell type, the pathological environment, and specific signaling pathways [22]. For instance, In degenerative disc disease, increased CAV1 mediates the integrin β1 and NF-κB signaling pathways to facilitate IL-1β-induced cellular inflammation [63]. Conversely, in non-alcoholic fatty liver disease (NAFLD), CAV1 alleviates inflammation by targeting angiotensin II (Ang II) [64]. Extracellular matrix protein-3 enters astrocytes via caveolin-1-mediated endocytosis, binds to NF-κB p65, and translocates into the nucleus, thereby suppressing the transcription of inflammatory factors [65]. In these settings, CAV1 knockdown might alter endocytic recycling, thereby promoting inflammatory cascades. Further studies are warranted to elucidate these mechanisms.

Neuron-glia crosstalk contributes to the mechanisms underlying pain conditions [20]. Within the CNS, neurons and microglia communicate via direct and indirect interactions: the former involves physical membrane contact between the two cell types, whereas the latter relies on soluble mediators such as cytokines, growth factors, or even neurotransmitters to mediate intercellular signaling [66]. Our results demonstrated that neuronal CAV1 overexpression significantly reduced the expression levels of TNFα and IL-1β in microglia, suggesting that CAV1 upregulation effectively suppresses microglia-mediated inflammatory responses. This is likely to indirectly regulate microglial function by modulating the release of neurotransmitters and other mediators from neurons. There are several signaling pathways are involved in soluble factor-dependent microglia-neuron interaction, including BDNF/TrkB signaling, IL-6 trans-signaling, and extracellular vesicle (EV) shedding [66]. The communication between microglia and neurons in the CNS is a complex process that involves a wide range of intermediate organs/cells, soluble factors, and membrane-to-membrane contact. Further studies are required to elucidate the precise mechanisms underlying the crosstalk between CAV1-modulated neurons and microglia.

CGRP receptor antagonists, such as gepants and monoclonal antibodies, are currently used to treat migraine by blocking the binding of CGRP to its receptor complex, thereby inhibiting receptor activation. However, like other GPCRs, long-term use of these drugs may lead to receptor upregulation [67]. CLR expression may increase compensatory in response to continuous inhibition by antagonists. This can result in rebound effects upon drug discontinuation. Directly degrading CLR, rather than merely blocking CGRP-CLR binding, could address issues related to drug tolerance and withdrawal reactions. This approach could also complement current CGRP/CLR-targeted therapies and provide new options for patients unresponsive to existing treatments. Despite significant challenges, CAV1 emerges as a promising new target due to its flexible regulatory role. Research on CAV1-based drug development is ongoing. Molecular

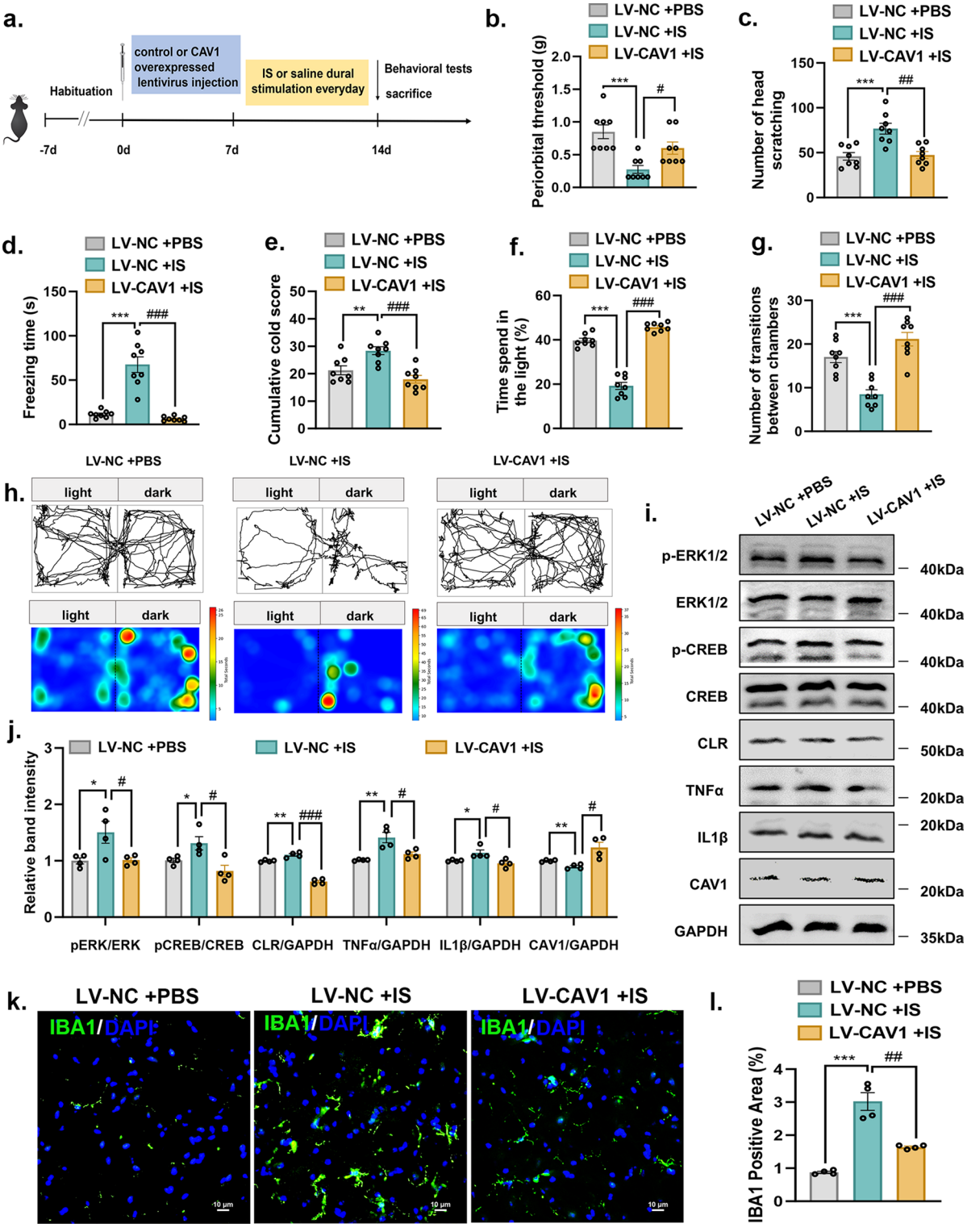

Fig. 8 CAV1 overexpression rescued the activation effects of CLR/ERK/CREB and microglia induced by IS stimulation in vivo. (**a**) Flow chart of the experimental design. (**b**-**h**) Migraine-like behaviors, including periorbital threshold (b), number of head scratching (**c**), freezing time (**d**), cold pain scores (**e**), time spent in the light (**f**), number of transitions between chambers (**i**), representative movement traces and heatmaps of the mice in the light/dark box (**h**) were assessed after CAV1 overexpression on migraine mice. $n = 8$ mice per group. (**i**-**j**) Representative immunoblots and CLR/ERK/CREB signaling quantification and TNFα/IL1β in the TNC after CAV1 overexpression on migraine mice. $n = 4$ mice per group. (**k**-**l**) Representative immunofluorescence images and quantification of IBA1 in the TNC after CAV1 overexpression on migraine mice. Scale bar: 10 μm. $n = 4$ mice per group. Mean ± SEM, One-way ANOVA, $^{*}p < 0.05$, $^{*}p < 0.01$ and $^{*}p < 0.001$ compared with LV-NC + PBS group, $^{\#}p < 0.05$, $^{\#}p < 0.01$ and $^{\#\#\#}p < 0.001$ compared with LV-NC + IS group. *Abbreviations: CAV1: caveolin-1; CLR: calcitonin receptor-like receptor; TNC: trigeminal nucleus caudalis; LV: lentivirus; NC: normal control*

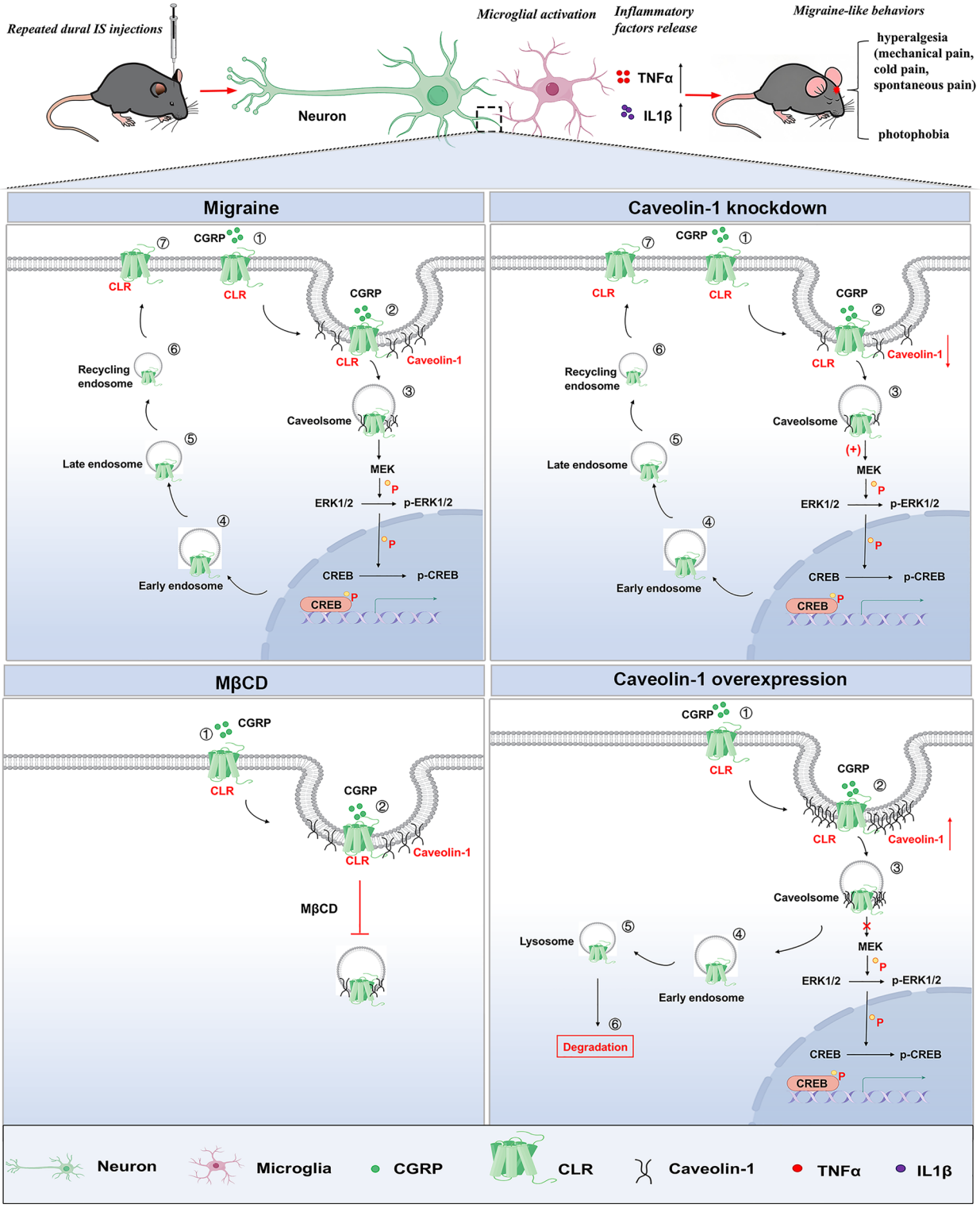

Fig. 9 (See legend on next page.)

(See figure on previous page.)

Fig. 9 Schematic diagram for the mechanisms of targeting CAV1 in treating migraines. Repeated IS stimulation in female mice induces CGRP release, activating CLR and triggering its internalization. CAV1 expression is downregulated in the TNC. CAV1 directly interacts with CLR and modulates its intracellular trafficking. This cascade upregulates CLR expression and concomitant activation of the ERK/CREB signaling axis and microglia. Activated microglia subsequently release TNFα and IL-1β, culminating in migraine-like behaviors (hyperalgesia, photophobia). Direct knockdown of CAV1 in the TNC of female mice amplifies CGRP/CLR signaling, reinforcing ERK/CREB and microglial activation to exacerbate neuroinflammation and migraine-related behavioral phenotypes. Pharmacological disruption of caveolae by MβCD impedes CLR internalization, leading to concurrent attenuation of ERK/CREB activation and neuroinflammatory processes, collectively ameliorate migraine symptoms. CAV1 overexpression promotes CLR internalization and degradation, reducing CGRP levels and mitigating ERK/CREB activation and neuroinflammation, ultimately reversing IS-induced migraine behaviors. *Abbreviations: CAV1: caveolin-1 TNC: trigeminal nucleus caudalis; CLR: calcitonin receptor-like receptor; MβCD: methyl-β-cyclodextrin*

glue might be helpful in binding CAV1 to target proteins, promoting drug internalization, and enhancing therapeutic efficacy [17, 68].

Nevertheless, there are several limitations to be considered. Firstly, despite migraine occurring frequently in women, the role of CAV1 in male mice still requires further investigation. Secondly, more in-depth studies of other established migraine animal models and patients are needed to generalize these findings. Thirdly, since CAV1 plays a role in diverse biological processes, further studies are required to better define the optimal dosing strategy for CAV1. Fourthly, adrenomedullin receptors CLR/RAMP2 (AM1 receptor) and CLR/RAMP3 (AM2) are expressed in migraine-related regions [69], such as the trigeminal ganglion and dorsal root ganglia. Moreover, Our study does not explore the potential interplay between CAV1 and RAMP1, a critical component of the functional CGRP receptor [9]. Future work should investigate whether CAV1 concurrently regulates RAMP1 trafficking or modulates receptor stoichiometry under migraine-related conditions.

Conclusions

In summary, we demonstrated that CAV1 negatively regulates CLR expression, inhibiting the ERK/CREB pathway and microglia-mediated neuroinflammation, alleviating migraine-like behaviors in a well-established female migraine model. Targeting CAV1 may provide a complementary therapeutic strategy for migraine treatment.

Abbreviations

Ang II	Angiotensin II
ANOVA	Analysis Of Variance
CAV1	Caveolin-1
CGRP	Calcitonin Gene-Related Peptide
CLR	Calcitonin Receptor-Like Receptor
coIP	co-Immunoprecipitation
ECL	Enhanced Chemiluminescence
EV	Extracellular Vesicle
FBS	Fetal Bovine Serum
GBD	Global Burden Disease
GPCR	G-Protein-Coupled Receptor
GRKs	G protein-coupled Receptor Kinases
IS	Inflammatory Soup
KO	Knock-Out
LV	Lentivirus
mIHC	multiplex Immunohistochemistry staining
MOI	Multiplicity Of Infection
MβCD	Methyl-β-Cyclodextrin
NAFLD	Non-Alcoholic Fatty Liver Disease
NC	Normal Control
PBS	Phosphate Buffer Saline
PMSF	Phenylmethylsulfonyl Fluoride
PVDF	Polyvinylidene-Difluoride
RAMP1	Receptor Activity Modifying Protein 1
si	siRNA
TNC	Trigeminal Nucleus Caudalis
VEH	Vehicle
WB	Western Blot

Supplementary Information

The online version contains supplementary material available at https://doi.org/10.1186/s12974-025-03466-8.

Supplementary Material 1

Supplementary Material 2

Acknowledgements

The authors would like to thank the Central Laboratory, Renmin Hospital of Wuhan University (Wuhan, China) for providing relevant experimental facilities and technical support.

Author contributions

Y.J. Zhou and W. Chen designed and performed the majority of the research work; Y.J. Zhou, Y. Zhang, L.Y. and F. Lu contributed to manuscript revisions and addressing reviewer comments; W. Yan performed experiments and tissue harvesting; Q.F. Xie and Y. Huang contributed to data collection and behavioral tests; Y, Zhang and W.B. Huang contributed to microinjection experiments; L.T. Wang and Z.M. Zeng analyzed the data. Y.J. Zhou wrote the manuscript. Z.M. Xiao guided the completion of this article. All authors read and approved the final manuscript.

Funding

This work was supported by grants from the National Natural Science Foundation of China (81971055,81471133, 82101292), the Natural Science Foundation of Hubei Province (no. 2020CFB226), and BUCA Research Fund Grant Program (HIGHER2022094). The authors declare no conflict of interest.

Data availability

No datasets were generated or analysed during the current study.

Declarations

Ethics approval and consent to participate

Experimental procedures were approved by the Institutional Animal Care and Use Committee (IACUC) of Renmin Hospital of Wuhan University.

Consent for publication

Not applicable.

Competing interests

The authors declare no competing interests.

Received: 19 October 2024 / Accepted: 10 May 2025
Published online: 21 May 2025

References

1. Headache Classification Committee of the International Headache Society (IHS). The International Classification of Headache Disorders, 3rd edition. Cephalalgia 2018;38:1–211. https://doi.org/10.1177/0333102417738202
2. Cen J, Wang Q, Cheng L, Gao Q, Wang H, Sun F. Global, regional, and National burden and trends of migraine among women of childbearing age from 1990 to 2021: insights from the global burden of disease study 2021. J Headache Pain. 2024;25:96. https://doi.org/10.1186/s10194-024-01798-z.
3. GBD 2021 Nervous System Disorders Collaborators. Global, regional, and National burden of disorders affecting the nervous system, 1990–2021: a systematic analysis for the global burden of disease study 2021. Lancet Neurol. 2024;23:344–81. https://doi.org/10.1016/S1474-4422(24)00038-3.
4. de Dios A, Pagès-Puigdemont N, Ojeda S, Riera P, Pelegrín R, Morollon N, et al. Persistence, effectiveness, and tolerability of anti-calcitonin gene-related peptide monoclonal antibodies in patients with chronic migraine. Headache. 2024. https://doi.org/10.1111/head.14827.
5. Ornello R, Baldini F, Onofri A, Rosignoli C, De Santis F, Burgalassi A, et al. Impact of duration of chronic migraine on long-term effectiveness of monoclonal antibodies targeting the calcitonin gene-related peptide pathway-A real-world study. Headache. 2024. https://doi.org/10.1111/head.14788.
6. Egea SC, Dickerson IM. Direct interactions between Calcitonin-Like receptor (CLR) and CGRP-Receptor component protein (RCP) regulate CGRP receptor signaling. Endocrinology. 2012;153:1850–60. https://doi.org/10.1210/en.2011-1459.
7. CGRP as the target of. new migraine therapies — successful translation from bench to clinic| Nature Reviews Neurology n.d. https://www.nature.com/articles/s41582-018-0003-1 (accessed December 14, 2023).
8. Cottrell GS, Padilla B, Pikios S, Roosterman D, Steinhoff M, Grady EF, et al. Post-endocytic sorting of calcitonin receptor-like receptor and receptor activity-modifying protein 1. J Biol Chem. 2007;282:12260–71. https://doi.org/10.1074/jbc.M606338200.
9. Hilairet S, Bélanger C, Bertrand J, Laperrière A, Foord SM, Bouvier M. Agonist-promoted internalization of a ternary complex between calcitonin receptor-like receptor, receptor activity-modifying protein 1 (RAMP1), and beta-arrestin. J Biol Chem. 2001;276:42182–90. https://doi.org/10.1074/jbc.M107323200.
10. Mode and site of action of therapies targeting CGRP signaling - PubMed. n.d. https://pubmed.ncbi.nlm.nih.gov/37691118/ (accessed February 15, 2025).
11. Lim JE, Bernatchez P, Nabi IR. Scaffolds and the scaffolding domain: an alternative paradigm for caveolin-1 signaling. Biochem Soc Trans. 2024;52:947–59. https://doi.org/10.1042/BST20231570.
12. Huang Q, Zhong W, Hu Z, Tang X. A review of the role of cav-1 in neuropathology and neural recovery after ischemic stroke. J Neuroinflammation. 2018;15:348. https://doi.org/10.1186/s12974-018-1387-y.
13. Potential of caveolae. in the therapy of cardiovascular and neurological diseases - PubMed n.d. https://pubmed.ncbi.nlm.nih.gov/25324780/ (accessed September 30, 2024).
14. Ostrom RS, Insel PA. The evolving role of lipid rafts and caveolae in G protein-coupled receptor signaling: implications for molecular Pharmacology. Br J Pharmacol. 2004;143:235–45. https://doi.org/10.1038/sj.bjp.0705930.
15. Barnett-Norris J, Lynch D, Reggio PH. Lipids, lipid rafts and caveolae: their importance for GPCR signaling and their centrality to the endocannabinoid system. Life Sci. 2005;77:1625–39. https://doi.org/10.1016/j.lfs.2005.05.040.
16. Ginés S, Ciruela F, Burgueño J, Casadó V, Canela EI, Mallol J, et al. Involvement of Caveolin in ligand-induced recruitment and internalization of A(1) adenosine receptor and adenosine deaminase in an epithelial cell line. Mol Pharmacol. 2001;59:1314–23.
17. Simón L, Campos A, Leyton L, Quest AFG. Caveolin-1 function at the plasma membrane and in intracellular compartments in cancer. Cancer Metastasis Rev. 2020;39:435–53. https://doi.org/10.1007/s10555-020-09890-x.
18. Mineo C, James GL, Smart EJ, Anderson RG. Localization of epidermal growth factor-stimulated Ras/Raf-1 interaction to caveolae membrane. J Biol Chem. 1996;271:11930–5. https://doi.org/10.1074/jbc.271.20.11930.
19. Shvets E, Bitsikas V, Howard G, Hansen CG, Nichols BJ. Dynamic caveolae exclude bulk membrane proteins and are required for sorting of excess glycosphingolipids. Nat Commun. 2015;6:6867. https://doi.org/10.1038/ncomms7867.
20. Zhou Y, Zhang L, Hao Y, Yang L, Fan S, Xiao Z. FKN/CX3CR1 axis facilitates migraine-Like behaviour by activating thalamic-cortical network microglia in status epilepticus model rats. J Headache Pain. 2022;23:42. https://doi.org/10.1186/s10194-022-01416-w.
21. Qiu T, Zhou Y, Hu L, Shan Z, Zhang Y, Fang Y, et al. 2-Deoxyglucose alleviates migraine-related behaviors by modulating microglial inflammatory factors in experimental model of migraine. Front Neurol. 2023;14:1115318. https://doi.org/10.3389/fneur.2023.1115318.
22. Badaut J, Blochet C, Obenaus A, Hirt L. Physiological and pathological roles of Caveolins in the central nervous system. Trends Neurosci. 2024;47:651–64. https://doi.org/10.1016/j.tins.2024.06.003.
23. Niesman IR, Schilling JM, Shapiro LA, Kellerhals SE, Bonds JA, Kleschevnikov AM, et al. Traumatic brain injury enhances neuroinflammation and lesion volume in Caveolin deficient mice. J Neuroinflamm. 2014;11:39. https://doi.org/10.1186/1742-2094-11-39.
24. Cellular prion protein acts. as mediator of amyloid beta uptake by caveolin-1 causing cellular dysfunctions in vitro and in vivo - da Silva Correia - Alzheimer's & Dementia - Wiley Online Library n.d. https://alz-journals.onlinelibrary.wiley.com/doi/10.1002/alz.14120 (accessed October 4, 2024).
25. Shan Z, Wang Y, Qiu T, Zhou Y, Zhang Y, Hu L, et al. SS-31 alleviated nociceptive responses and restored mitochondrial function in a headache mouse model via Sirt3/Pgc-1α positive feedback loop. J Headache Pain. 2023;24:65. https://doi.org/10.1186/s10194-023-01600-6.
26. Cui H, Su W, Cao Y, Ma L, Xu G, Mou W, et al. Lack of spinal neuropeptide Y is involved in mechanical itch in aged mice. Front Aging Neurosci. 2021;13:654761. https://doi.org/10.3389/fnagi.2021.654761.
27. Edelmayer RM, Vanderah TW, Majuta L, Zhang E-T, Fioravanti B, De Felice M, et al. Medullary pain facilitating neurons mediate allodynia in headache-related pain. Ann Neurol. 2009;65:184–93. https://doi.org/10.1002/ana.21537.
28. Pi C, Tang W, Li Z, Liu Y, Jing Q, Dai W, et al. Cortical pain induced by optogenetic cortical spreading depression: from whole brain activity mapping. Mol Brain. 2022;15:99. https://doi.org/10.1186/s13041-022-00985-w.
29. Chugh G, Asghar M, Patki G, Bohat R, Jafri F, Allam F, et al. A High-Salt diet further impairs Age-Associated declines in cognitive, behavioral, and cardiovascular functions in male Fischer brown Norway Rats123. J Nutr. 2013;143:1406–13. https://doi.org/10.3945/jn.113.177980.
30. Xie L-Q, Hu B, Lu R-B, Cheng Y-L, Chen X, Wen J, et al. Raptin, a sleep-induced hypothalamic hormone, suppresses appetite and obesity. Cell Res. 2025. https://doi.org/10.1038/s41422-025-01078-8.
31. MβCD inhibits SFTSV entry. by disrupting lipid raft structure of the host cells - PubMed n.d. https://pubmed.ncbi.nlm.nih.gov/39265655/ (accessed February 17, 2025).
32. Grimmer S, Iversen T-G, van Deurs B, Sandvig K. Endosome to golgi transport of ricin is regulated by cholesterol. Mol Biol Cell. 2000;11:4205–16.
33. Long-term safety. of zavegepant nasal spray for the acute treatment of migraine: A phase 2/3 open-label study - PubMed n.d. https://pubmed.ncbi.nlm.nih.gov/39210835/ (accessed September 29, 2024).
34. Kashyap K, Shukla R. Drug delivery and targeting to the brain through nasal route: mechanisms, applications and challenges. Curr Drug Deliv. 2019;16:887–901. https://doi.org/10.2174/1567201816666191029122740.
35. Inhibiting PAC1 receptor internalization and endosomal ERK pathway activation may ameliorate hyperalgesia in a chronic migraine rat model - Lily Zhang, Yanjie Zhou, Yajuan Wang, Liu Yang, Yue Wang, Zhengming Shan, Jingjing Liang, Zheman Xiao. 2023 n.d. https://journals.sagepub.com/doi/10.1177/03331024231163131 (accessed September 29, 2024).
36. Tian R, Zhang Y, Pan Q, Wang Y, Wen Q, Fan X, et al. Calcitonin gene-related peptide receptor antagonist BIBN4096BS regulates synaptic transmission in the vestibular nucleus and improves vestibular function via PKC/ERK/CREB pathway in an experimental chronic migraine rat model. J Headache Pain. 2022;23:35. https://doi.org/10.1186/s10194-022-01403-1.
37. Vavolizza RD, Petroni GR, Mauldin IS, Chianese-Bullock KA, Olson WC, Smith KT, et al. Phase I/II clinical trial of a helper peptide vaccine plus PD-1 Blockade in PD-1 antibody-naïve and PD-1 antibody-experienced patients with melanoma (MEL64). J Immunother Cancer. 2022;10:e005424. https://doi.org/10.1136/jitc-2022-005424.
38. Yu H, Cui X, Zhang J, Xie JX, Banerjee M, Pierre SV, et al. Heterogeneity of signal transduction by Na-K-ATPase α-isoforms: role of Src interaction. Am J Physiol Cell Physiol. 2018;314:C202–10. https://doi.org/10.1152/ajpcell.00124.2017.
39. Sudhahar V, Okur MN, O'Bryan JP, Minshall RD, Fulton D, Ushio-Fukai M, et al. Caveolin-1 stabilizes ATP7A, a copper transporter for extracellular SOD, in

vascular tissue to maintain endothelial function. Am J Physiol Cell Physiol. 2020;319:C933–44. https://doi.org/10.1152/ajpcell.00151.2020.
40. Wright SC, Lukasheva V, Le Gouill C, Kobayashi H, Breton B, Mailhot-Larouche S, et al. BRET-based effector membrane translocation assay monitors GPCR-promoted and endocytosis-mediated Gq activation at early endosomes. Proc Natl Acad Sci U S A. 2021;118:e2025846118. https://doi.org/10.1073/pnas.2025846118.
41. Armstrong SM, Sugiyama MG, Fung KYY, Gao Y, Wang C, Levy AS, et al. A novel assay uncovers an unexpected role for SR-BI in LDL transcytosis. Cardiovasc Res. 2015;108:268–77. https://doi.org/10.1093/cvr/cvv218.
42. Lim S, Kim W-J, Kim Y-H, Lee S, Koo J-H, Lee J-A, et al. dNP2 is a blood–brain barrier-permeable peptide enabling ctCTLA-4 protein delivery to ameliorate experimental autoimmune encephalomyelitis. Nat Commun. 2015;6:8244. https://doi.org/10.1038/ncomms9244.
43. Huang W, Zhang Y, Zhou Y, Zong J, Qiu T, Hu L, et al. Glymphatic dysfunction in migraine mice model. Neuroscience. 2023;528:64–74. https://doi.org/10.1016/j.neuroscience.2023.07.027.
44. Codenotti S, Faggi F, Ronca R, Chiodelli P, Grillo E, Guescini M, et al. Caveolin-1 enhances metastasis formation in a human model of embryonal rhabdomyosarcoma through Erk signaling Cooperation. Cancer Lett. 2019;449:135–44. https://doi.org/10.1016/j.canlet.2019.02.013.
45. Edvinsson L. The trigeminovascular pathway: role of CGRP and CGRP receptors in migraine. Headache. 2017;57(Suppl 2):47–55. https://doi.org/10.1111/head.13081.
46. Iyengar S, Johnson KW, Ossipov MH, Aurora SK. CGRP and the trigeminal system in migraine. Headache: J Head Face Pain. 2019;59:659–81. https://doi.org/10.1111/head.13529.
47. Neeb L, Hellen P, Boehnke C, Hoffmann J, Schuh-Hofer S, Dirnagl U, et al. IL-1β stimulates COX-2 dependent PGE2 synthesis and CGRP release in rat trigeminal ganglia cells. PLoS ONE. 2011;6:e17360. https://doi.org/10.1371/journal.pone.0017360.
48. Meng J, Wang J, Steinhoff M, Dolly JO. TNFα induces co-trafficking of TRPV1/TRPA1 in VAMP1-containing vesicles to the plasmalemma via Munc18-1/syntaxin1/SNAP-25 mediated fusion. Sci Rep. 2016;6:21226. https://doi.org/10.1038/srep21226.
49. Yarwood RE, Imlach WL, Lieu T, Veldhuis NA, Jensen DD, Klein Herenbrink C, et al. Endosomal signaling of the receptor for calcitonin gene-related peptide mediates pain transmission. Proc Natl Acad Sci U S A. 2017;114:12309–14. https://doi.org/10.1073/pnas.1706656114.
50. Walker CS, Raddant AC, Woolley MJ, Russo AF, Hay DL. CGRP receptor antagonist activity of olcegepant depends on the signalling pathway measured. Cephalalgia. 2018;38:437–51. https://doi.org/10.1177/0333102417691762.
51. Dalton CM, Schlegel C, Hunter CJ. Caveolin-1: A review of intracellular functions, tissue-specific roles, and epithelial tight junction regulation. Biology (Basel). 2023;12:1402. https://doi.org/10.3390/biology12111402.
52. Štefl M, Takamiya M, Middel V, Tekpınar M, Nienhaus K, Beil T, et al. Caveolae disassemble upon membrane lesioning and foster cell survival. iScience. 2024;27:108849. https://doi.org/10.1016/j.isci.2024.108849.
53. Le Roy C, Wrana JL. Clathrin- and non-clathrin-mediated endocytic regulation of cell signalling. Nat Rev Mol Cell Biol. 2005;6:112–26. https://doi.org/10.1038/nrm1571.
54. Tang JQ, Sun F, Wang YH, Chen LX, Yao CH, Fu XQ, et al. The role of caveolae in regulating calcitonin receptor-like receptor subcellular distribution in vascular smooth muscle cells. Biochem Cell Biol. 2013;91:357–60. https://doi.org/10.1139/bcb-2013-0020.
55. Kuwasako K, Shimekake Y, Masuda M, Nakahara K, Yoshida T, Kitaura M, et al. Visualization of the calcitonin receptor-like receptor and its receptor activity-modifying proteins during internalization and recycling. J Biol Chem. 2000;275:29602–9. https://doi.org/10.1074/jbc.M004534200.
56. Chen Y-G. Endocytic regulation of TGF-beta signaling. Cell Res. 2009;19:58–70. https://doi.org/10.1038/cr.2008.315.
57. Nascimento RB, Risteli M, Paiva KBS, Juurikka K, Rodrigues MFSD, Salo TA, et al. Cholesterol depletion affects caveolin-1 expression, migration and invasion of oral tongue squamous cell carcinoma cell lines. Arch Oral Biol. 2023;150:105675. https://doi.org/10.1016/j.archoralbio.2023.105675.
58. Li S, Xiao D, Zhao Y, Zhang L, Chen R, Liu W, et al. Porcine deltacoronavirus (PDCoV) entry into PK-15 cells by caveolae-mediated endocytosis. Viruses. 2022;14:496. https://doi.org/10.3390/v14030496.
59. Ekdahl CT, Kokaia Z, Lindvall O. Brain inflammation and adult neurogenesis: the dual role of microglia. Neuroscience. 2009;158:1021–9. https://doi.org/10.1016/j.neuroscience.2008.06.052.
60. Stevens B, Allen NJ, Vazquez LE, Howell GR, Christopherson KS, Nouri N, et al. The classical complement cascade mediates CNS synapse elimination. Cell. 2007;131:1164–78. https://doi.org/10.1016/j.cell.2007.10.036.
61. Zhao H, Lv Y, Xu J, Song X, Wang Q, Zhai X, et al. The activation of microglia by the complement system in neurodegenerative diseases. Ageing Res Rev. 2025;104:102636. https://doi.org/10.1016/j.arr.2024.102636.
62. Cao D, Li B, Cao C, Zhang J, Li X, Li H, et al. Caveolin-1 aggravates neurological deficits by activating neuroinflammation following experimental intracerebral hemorrhage in rats. Exp Neurol. 2023;368:114508. https://doi.org/10.1016/j.expneurol.2023.114508.
63. Zhang W, Wang H, Yuan Z, Chu G, Sun H, Yu Z, et al. Moderate mechanical stimulation rescues degenerative annulus fibrosus by suppressing caveolin-1 mediated pro-inflammatory signaling pathway. Int J Biol Sci. 2021;17:1395–412. https://doi.org/10.7150/ijbs.57774.
64. Fu D, Wu S, Jiang X, You T, Li Y, Xin J, et al. Caveolin-1 alleviates acetaminophen-induced vascular oxidative stress and inflammation in non-alcoholic fatty liver disease. Free Radic Biol Med. 2023;195:245–57. https://doi.org/10.1016/j.freeradbiomed.2022.12.095.
65. Matrilin-3 supports neuroprotection in ischemic stroke by suppressing astrocyte-mediated neuroinflammation - PubMed n.d. https://pubmed.ncbi.nlm.nih.gov/38520693/ (accessed February 23, 2025).
66. Hu Y, Tao W. Current perspectives on microglia-neuron communication in the central nervous system: direct and indirect modes of interaction. J Adv Res. 2024;66:251–65. https://doi.org/10.1016/j.jare.2024.01.006.
67. Altarifi AA, David B, Muchhala KH, Blough BE, Akbarali H, Negus SS. Effects of acute and repeated treatment with the biased mu opioid receptor agonist TRV130 (oliceridine) on measures of antinociception, Gastrointestinal function, and abuse liability in rodents. J Psychopharmacol. 2017;31:730–9. https://doi.org/10.1177/0269881116689257.
68. Wang H, Wang H, Wang R, Li Y, Wang Z, Zhou W, et al. Discovery of a molecular glue for EGFR degradation. Oncogene. 2025;44:545–56. https://doi.org/10.1038/s41388-024-03241-8.
69. Edvinsson L, Grell A-S, Warfvinge K. Expression of the CGRP family of neuropeptides and their receptors in the trigeminal ganglion. J Mol Neurosci. 2020;70:930–44. https://doi.org/10.1007/s12031-020-01493-z.

Publisher's note